THE JOURNAL OF BIOLOGICAL CHEMISTRY VOL. 287, NO. 53, pp. 44447–44463, December 28, 2012

Lipid Raft-dependent Endocytosis of Close Homolog of Adhesion Molecule L1 (CHL1) Promotes Neuritogenesis*

Received for publication, June 24, 2012, and in revised form, October 24, 2012 Published, JBC Papers in Press, November 9, 2012, DOI 10.1074/jbc.M112.394973

Nan Tian[‡§1], Iryna Leshchyns'ka[‡¶1], Jeffrey H. Welch[¶], Witold Diakowski[‖], Hongyuan Yang[¶], Melitta Schachner[‡], and Vladimir Sytnyk[‡¶2]**

*From the [‡]Zentrum für Molekulare Neurobiologie, Universitätskrankenhaus Hamburg-Eppendorf, Martinistrasse 52, 20246 Hamburg, Germany, the [§]Department of Physiology, Dalian Medical University, 9 Western Lvshun South Road, Dalian 116044, China, the [‖]Laboratory of Cytobiochemistry, Biotechnology Faculty, University of Wrocław, Przybyszewskiego 63-77, 51-148 Wrocław, Poland, the **Keck Center for Collaborative Neuroscience and Department of Cell Biology and Neuroscience, Rutgers University, Piscataway, New Jersey 08854, and the [¶]School of Biotechnology and Biomolecular Sciences, University of New South Wales, Sydney, New South Wales 2052, Australia*

Background: Cell adhesion molecule CHL1 plays a dual role by either promoting or inhibiting neuritogenesis.
Results: Ligand-induced clustering of CHL1 at the cell surface induces lipid raft-dependent endocytosis of CHL1 and neuritogenesis.
Conclusion: Ligand-induced remodeling of CHL1 adhesion promotes neurite outgrowth.
Significance: High levels of CHL1 adhesion and inhibition of CHL1 endocytosis can interfere with neuronal development and/or regeneration.

CHL1 plays a dual role by either promoting or inhibiting neuritogenesis. We report here that neuritogenesis-promoting ligand-dependent cell surface clustering of CHL1 induces palmitoylation and lipid raft-dependent endocytosis of CHL1. We identify βII spectrin as a binding partner of CHL1, and we show that partial disruption of the complex between CHL1 and βII spectrin accompanies CHL1 endocytosis. Inhibition of the association of CHL1 with lipid rafts by pharmacological disruption of lipid rafts or by mutation of cysteine 1102 within the intracellular domain of CHL1 reduces endocytosis of CHL1. Endocytosis of CHL1 is also reduced by nifedipine, an inhibitor of the L-type voltage-dependent Ca^{2+} channels. CHL1-dependent neurite outgrowth is reduced by inhibitors of lipid raft assembly, inhibitors of voltage-dependent Ca^{2+} channels, and overexpression of CHL1 with mutated cysteine Cys-1102. Our results suggest that ligand-induced and lipid raft-dependent regulation of CHL1 adhesion via Ca^{2+}-dependent remodeling of the CHL1-βII spectrin complex and CHL1 endocytosis are required for CHL1-dependent neurite outgrowth.

Cell adhesion molecules mediate various interactions between cells and also between cells and the extracellular matrix in the developing and mature brain, and they are thus intimately involved in the regulation of brain development and function in the adult. The close homolog of L1 (CHL1)[3] is a cell adhesion molecule that belongs to the immunoglobulin superfamily due to the presence of six Ig-like domains in its extracellular part. CHL1 is highly expressed in neurons but is also detectable in astrocytes, oligodendrocytes, and Schwann cells (1). The extracellular domain of CHL1 binds to CHL1 molecules on adjacent membranes thereby mediating homophilic interactions (2). It also interacts with other adhesion molecules such as integrins (3) and NB-3, a member of the F3/contactin family of neural recognition molecules (4), and cell surface receptors, such as the receptor-type protein-tyrosine phosphatase α (4), semaphorin 3A receptor neuropilin 1 (5), and ephrin A5 receptor (6).

Binding of CHL1 to its ligands is associated with an increase in neuronal survival and differentiation (1, 7, 8). Mice constitutively deficient in CHL1 show abnormalities in brain structure, including loss of Purkinje and granule cells in the cerebellum, abnormal neuronal positioning and dendrite orientation in the cerebral cortex, and abnormal innervation of Purkinje cell dendrites by stellate axons in the cerebellar cortex (4, 9–11). In developing axons, CHL1 plays a role in axonal guidance by promoting the growth cone collapsing effects of semaphorin 3A (12). However, excessive CHL1-mediated adhesion limits neurite outgrowth and differentiation *in vitro* and *in vivo* (2). In agreement, ectodomain shedding of CHL1 by the metalloprotease-disintegrin ADAM8 promotes neurite outgrowth and suppresses neuronal cell death (13). Little is known, however, about how the levels of CHL1 at the cell surface are regulated.

An important role in the ability of CHL1 to promote neuronal differentiation is played by the cytoskeleton. CHL1 interacts with and recruits to the cell surface plasma membrane the cytoskeleton-linker proteins such as ankyrin and the ezrin-radixin-

* This work was supported by Deutsche Forschungsgemeinschaft (to M. S., I. L., and V. S.), The Rebecca L. Cooper Medical Research Foundation (to V. S. and I. L.), National Health and Medical Research Council (to V. S.), and the New Jersey Commission for Spinal Cord Research (to M. S.).
[1] Both authors contributed equally to this work.
[2] To whom correspondence should be addressed: School of Biotechnology and Biomolecular Sciences, University of New South Wales, Sydney, New South Wales 2052, Australia. Tel.: 61-2-93851108; Fax: 61-2-93851483; E-mail: v.sytnyk@unsw.edu.au.

[3] The abbreviations used are: CHL1, close homolog of L1; NB-DNJ, *N*-butyldeoxynojirimycin; NCAM, neural cell adhesion molecule; VDCC, voltage-dependent Ca^{2+} channel; ANOVA, analysis of variance; TfR, transferrin receptor; ID, intracellular domain.

moesin (ERM) family of proteins (3, 12). Mutations in the ankyrin- and ERM-binding motifs abrogate the ability of CHL1 to promote neuronal migration and neurite outgrowth (3, 12). How the association of CHL1 with the cytoskeleton is regulated remains poorly understood.

In this study, we show that CHL1 directly associates with βII spectrin, and we demonstrate that ligand-induced clustering of CHL1 induces palmitoylation of CHL1 and lipid raft-dependent remodeling of the CHL1-βII spectrin complex, accompanied by CHL1 endocytosis, which are required for CHL1-dependent neurite outgrowth.

EXPERIMENTAL PROCEDURES

Antibodies and Toxins—Rabbit polyclonal antibodies (14) and goat polyclonal antibodies (R&D Systems, Minneapolis, MN) against the extracellular domain of CHL1 were used for Western blot analysis, immunocytochemistry, and assay for neurite outgrowth showing similar results. Monoclonal antibody 2C2 reacting with the cytoplasmic domains of L1 and CHL1 (15) was used in *in vitro* protein binding assays. Goat polyclonal antibodies against the intracellular domain of CHL1 (Santa Cruz Biotechnology) were used in the proximity ligation assay. Mouse monoclonal antibodies against βII spectrin, ankyrin-B, and clathrin heavy chain were from BD Biosciences; nonimmune antibodies and rabbit polyclonal antibodies against $p59^{Fyn}$ and βII spectrin were from Santa Cruz Biotechnology; rabbit polyclonal antibodies against actin and βI spectrin were from Sigma; mouse monoclonal antibodies against Na^+/K^+-ATPase (α6F) were from Developmental Studies Hybridoma Bank (University of Iowa, IA); polyclonal goat antibodies against F3/F11/contactin-1 were from R&D Systems (Minneapolis, MN); and mouse monoclonal antibodies against transferrin receptors were from Invitrogen. Secondary antibodies against rabbit, goat, and mouse Ig-coupled to horseradish peroxidase (HRP), cy2, cy3, or cy5 were from Jackson ImmunoResearch. Methyl-β-cyclodextrin and lipid biosynthesis inhibitors mevastatin, mevinolin, *N*-butyldeoxynojirimycin (NB-DNJ), and fumonisin B were from Sigma. Voltage-dependent Ca^{2+} channel blockers nifedipine and pimozide were from Alomone Laboratories (Jerusalem, Israel).

Animals—In this study 1- to 3-day-old wild type C57BL/6J and CHL1-deficient ($CHL1^{-/-}$) mice (16) were used. $CHL1^{-/-}$ mice had been back-crossed onto a C57BL/6J genetic background for 10 generations. All experiments were approved by the Animal Care and Ethics Committee of the University of New South Wales.

DNA Constructs and siRNA—To clone CHL1, double-stranded cDNA was synthesized using SuperScript™ II RT (Invitrogen) from total RNA isolated from mouse brain by the High Pure RNA tissue kit (Roche Diagnostics). Mouse CHL1 was amplified from cDNA and cloned into pcDNA™ 3.1/V5-His vector using corresponding TOPO expression kit (Invitrogen) according to the manufacturer's instructions. Plasmid DNA containing full-length CHL1 in pcDNA3.1 was taken as template for subcloning and site-directed mutagenesis. pEF/FRT/V5-D-TOPO cloning kit (Invitrogen) was used to generate the expression construct encoding full-length CHL1, which was used for transfection. Single amino acid change was made using the QuikChange II XL site-directed mutagenesis kit from Stratagene (La Jolla, CA) according to the manufacturer's protocol. The following primers were used to generate the C1102S mutation within the CHL1 intracellular domain: forward primer, 5′-ACACTGATATTGTTAACTATTTCCTTTGTGAAGAGGAACAGAGGT-3′, and reverse primer 5′-ACCTCTGTTCCTCTTCACAAAGGAAATAGTTAACAATATCAGTGT-3′. Control nonsilencing and βII spectrin siRNA were from Qiagen. Transfection with βII spectrin siRNA (target sequence AAGGTGCTTGATAATGCTATA) reduced by ~50% the expression of βII spectrin at 24 h after transfection as verified by Western blot analysis (data not shown) and immunocytochemistry (Fig. 9*B*), allowing it to be used as functional βII spectrin siRNA. The βII spectrin siRNA (target sequence AACCATCATCATCCTAAACAA) did not affect βII spectrin expression as verified by Western blot analysis and immunocytochemistry and was used as nonfunctional siRNA control.

Cultures and Stable Transfection of NIH 3T3 Cells—Flp-In-NIH 3T3 cells (Invitrogen) were grown in DMEM/F-12 with 10% donor calf serum and 2% penicillin/streptomycin at 37 °C, 5% CO_2, and 90% relative humidity. Cells were passaged as they reached confluence. To generate stably transfected cell lines, cells were co-transfected with CHL1 pEF5/FRT/V5-D-TOPO and pOG44 plasmids using Lipofectamine 2000 reagent (Invitrogen) according to the manufacturer's instructions. The pOG44 plasmid expresses Flp recombinase, which helps the CHL1 cDNA to integrate into the genome of the 3T3 cells at the FRT site. Cells were selected in culture medium containing 200 μg/ml hygromycin B (Invitrogen) for 3–4 weeks. Single clones were isolated and verified by Western blot analysis.

Co-immunoprecipitation—For co-immunoprecipitation experiments, samples containing 1 mg of total protein were lysed for 20 min at 25 °C with lysis buffer (50 mM Tris-HCl, pH 7.5, 150 mM NaCl, 1% Nonidet P-40, 1 mM $Na_2P_2O_7$, 1 mM NaF) containing an EDTA-free protease inhibitor mixture (Roche Diagnostics). When indicated, 2 mM EGTA, 0.2 mM $CaCl_2$, or 2 mM $CaCl_2$ was added to the lysis buffer. Lysates were centrifuged at 20,000 × *g* for 15 min at 4 °C. The supernatants were precleared for 3 h at 4 °C with 20 μl of protein A-agarose beads per 1.5 ml of lysate under constant rotation. Beads were pelleted down by spinning at 500 × *g* for 5 min, and the supernatant was carefully pipetted out into another tube. The supernatants were incubated with polyclonal CHL1 antibodies or nonspecific rabbit immunoglobulins overnight at 4 °C with constant rotation, followed by incubation with protein A-agarose beads for 3 h at 4 °C. The beads were pelleted and washed four times with ice-cold lysis buffer. Proteins were eluted from the beads with Laemmli sample buffer and boiled at 100 °C for 10 min. The samples were analyzed by Western blot.

In Vitro Protein Binding Assay—Rabbit polyclonal antibodies against βII spectrin were used to immobilize βII spectrin. The antibodies (1 μg/ml in PBS) were adsorbed overnight to the plastic surface of 96-well MICROLON 600 plates (Greiner, Frickenhausen, Germany) at 4 °C. All steps were then performed at room temperature. Wells were blocked with 1% BSA in PBS for 1 h and incubated with purified mouse brain spectrin (6 μM) (17) for 1 h. Wells were washed and incubated for 1 h with increasing concentrations of CHL1-ID and L1-ID (15)

diluted in PBS with 1% BSA. Plates were washed five times with PBS containing 0.05% Tween 20 (PBST) and incubated for 1 h with the monoclonal antibody 2C2 reacting with the cytoplasmic domains of L1 and CHL1 (15) diluted 1:5,000 in PBST containing 1% BSA. After washing with PBST, wells were incubated for 1 h with HRP-coupled secondary antibodies in PBST containing 1% BSA, washed five times with PBST, and developed with 1 mg/ml *o*-phenylenediamine dihydrochloride (PerbioScience, Bonn, Germany). The absorbance was measured at 405 nm.

Isolation of Soluble, Total Membrane, and Lipid Raft Fractions—Brain homogenates were prepared using a Dounce homogenizer in a homogenization buffer (0.32 M sucrose, 1 mM $MgCl_2$, 1 mM $CaCl_2$, 1 mM $NaHCO_3$, 5 mM Tris, pH 7.4, protease inhibitor mixture (Roche Diagnostics)) and centrifuged at 700 × *g* for 10 min at 4 °C to pellet nuclei. The supernatants were centrifuged at 17,500 × *g* at 4 °C for 15 min. The supernatants were used as fractions enriched in soluble proteins, whereas pellets were used as total membrane fractions. Lipid rafts were isolated from the total membrane fraction as described (18). Membrane fraction (500 μl) was mixed with 4× volumes of ice-cold 1% Triton X-100 in TBS and incubated for 20 min on ice. Extracted membranes were mixed with an equal volume of 80% sucrose in 0.2 M Na_2CO_3 to a final sucrose concentration of 40%. To create a discontinuous gradient, this 40% sucrose solution was overlaid with 2 ml of 30% sucrose in TBS and 1 ml of 10% sucrose in TBS. Tubes were filled to capacity with TBS and centrifuged at 230,000 × *g* for 17 h. Lipid rafts were collected at the top of the gradient at 10% sucrose, resuspended in TBS, and pelleted down by centrifugation at 100,000 × *g* for 1 h. The pellets were resuspended in TBS containing protease inhibitor mixture. To estimate the fraction of CHL1, ankyrin-B, and βII spectrin in lipid rafts, enrichment of these proteins in lipid rafts *versus* brain homogenate was compared with the enrichment of contactin-1, which localizes exclusively to lipid rafts as shown in Equation 1,

$$\text{LR fraction (protein of interest)} = I_{LR}(\text{protein of interest})/I_{BH}(\text{protein of interest}) \times I_{BH}(\text{contactin-1})/I_{LR}(\text{contactin-1}) \times 100\% \quad \text{(Eq. 1)}$$

where I_{LR} and I_{BH} are levels in lipid rafts and brain homogenates as estimated by Western blot analysis. Similar estimations were obtained using Fyn as a lipid raft reference protein (data not shown).

Analysis of Spectrin Meshwork Polymerization—Isolation of 0.1% Triton X-100-soluble and -insoluble proteins was performed as described (19). Brain homogenates were extracted for 5 min at 4 °C with PHEM buffer (60 mM Pipes, 25 mM HEPES, 10 mM EGTA, 2 mM $MgCl_2$, pH 6.9) containing 0.1% Triton X-100 and protease inhibitor mixture. Samples were then centrifuged for 10 min at 48,000 × *g* at 4 °C. Supernatants containing nonpolymerized proteins and pellets containing polymerized spectrin meshwork were analyzed by Western blot.

Isolation of the Cell Surface Proteins by Biotinylation—CHL1 constructs were transiently transfected into 3T3 cells grown in 6-well dishes using Lipofectamine 2000. Twenty four hours after transfection, polyclonal antibodies against the extracellular domain of CHL1 (1:200) were applied to cells for 10 min at 37 °C. To block VDCC, 10 μM nifedipine and 5 μM pimozide were applied for 10 min at 37 °C before antibody application. The cells were washed twice with ice-cold PBS. Surface proteins were then biotinylated with 0.5 mg/ml of EZ-Link Sulfo-NHS-LC-Biotin (Pierce) applied for 30 min at 4 °C (20). The reactions were stopped by adding 50 mM glycine for 10 min at 4 °C. After washing twice with ice-cold PBS, the cells were scraped into 166 μl per well of warm precipitation buffer (PBS, 1% SDS, 5 mM EDTA, 5 mM EGTA) with the complete protease inhibitor mixture and phosphostop (Roche Diagnostics). This solution was then diluted with 833 μl per well of cold PBS containing 1% Triton X-100 and centrifuged at 20,000 × *g* for 20 min at 4 °C. To precipitate biotinylated proteins, supernatants containing equal amounts of the total protein were mixed with 100 μl of neutravidin-agarose beads (Pierce) overnight at 4 °C with rotation. After washing three times with PBST, the precipitates were boiled in Laemmli sample buffer and subjected to SDS-PAGE and Western blot analysis.

Neuronal Cultures—Hippocampal and cortical neurons were prepared from 1- to 3- day-old C57BL/6J mice and maintained for 24 h in Neurobasal A medium supplemented with 2% B-27 and GlutaMAX (Invitrogen) and FGF-2 (2 ng/ml, R&D Systems, Minneapolis, MN) on glass coverslips coated with poly-D-lysine (100 μg/ml) (21).

Neurite Outgrowth Assays—Neurite outgrowth was analyzed as described (22, 23). Briefly, for nontransfected neurons, polyclonal antibodies against the extracellular domain of CHL1 or nonspecific immunoglobulins were applied to the culture medium immediately after plating together with or without the lipid biosynthesis inhibitors mevinolin (4 μM), NB-DNJ (100 μM), or fumonisin B (50 μM) (24). When indicated, neurons were co-transfected with cherry (a kind gift of Dr. Tsien) and CHL1 cDNA constructs 6 h after plating using Lipofectamine 2000 (Invitrogen) combined with CombiMag (OzBiosciences, Marseille, France) according to the manufacturer's instructions. For transfected neurons, CHL1 antibodies and nonspecific immunoglobulins were applied 6 h after transfection. Neurons were fixed with 4% formaldehyde in PBS at 24 h after CHL1 antibody and nonspecific immunoglobulin application. The cells were imaged using an Axiophot 2 microscope equipped with a Plan-NeoFluar ×40 objective (numerical aperture 0.75), AxioCam HRc digital camera, and AxioVision software version 3.1 (Carl Zeiss, Oberkochen, Germany). Lengths of neurites were measured using ImageJ software (National Institute of Health, Bethesda). For each experimental value, at least 100 neurons with neurites longer than the cell body diameter were measured. Results were statistically evaluated using ANOVA.

Immunofluorescence Labeling—Indirect immunofluorescence labeling was performed as described previously (25). When indicated, live neurons were preincubated with goat polyclonal antibodies against CHL1 for 15 min in a CO_2 incubator at 37 °C to induce clustering of CHL1. Control neurons were treated with nonimmune immunoglobulins. Neurons were fixed in 4% formaldehyde in PBS, washed with PBS, permeabilized with 0.25% Triton X-100 in PBS for 5 min, and

blocked with 1% BSA in PBS for 20 min. Antibodies against CHL1 and βII spectrin were applied in 0.1% BSA in PBS overnight at 4 °C. Primary antibodies were detected with fluorochrome-coupled secondary antibodies applied for 60 min at room temperature. Immunofluorescence images were acquired at room temperature using a confocal laser scanning microscope LSM510, LSM510 software (version 3), and an oil Plan-NeoFluar ×63 objective (numerical aperture 1.3; all from Carl Zeiss) at ×3 digital zoom. Immunofluorescence intensity profiles were plotted in ImageJ.

Detergent Extraction of Cultured Neurons—Neurons were incubated with goat polyclonal antibodies against CHL1 or nonimmune immunoglobulins for 15 min in a CO_2 incubator at 37 °C either in the presence or absence of nifedipine (10 μM), then incubated for 1 min in cold microtubule stabilizing buffer (MSB: 2 mM $MgCl_2$, 10 mM EGTA, 60 mM PIPES, pH 7.0), and extracted for 8 min on ice with 1% Triton X-100 in MSB as described (18, 22). Neurons were then labeled with indirect immunofluorescence against CHL1 and βII spectrin as described under "Immunofluorescence Labeling" and co-labeled with fluorescent cholera toxin (5 μg/ml (18), Sigma) applied for 30 min at room temperature. Mean intensities of CHL1 and βII spectrin immunofluorescence were measured in ImageJ by automatically outlining GM1 clusters using a threshold function of ImageJ and measuring immunofluorescence intensities within the respective outlines.

Proximity Ligation Assay—Cultured neurons were fixed in 4% formaldehyde in PBS, washed with PBS, permeabilized with 0.25% Triton X-100 in PBS for 5 min, and blocked with 1% BSA in PBS for 20 min. Antibodies against βII spectrin and the intracellular domain of CHL1 were applied to the cells in 0.1% BSA in PBS overnight at 4 °C. Further steps were performed using secondary antibodies conjugated with oligonucleotides (PLA probes, Olink Bioscience, Uppsala, Sweden) and Duolink II fluorescence kit (Olink Bioscience) in accordance with the manufacturer's instructions. Fluorescence images were acquired at room temperature using a confocal laser scanning microscope Nikon C1si, NIS Elements software and oil Plan Apo VC ×60 objective (numerical aperture 1.4) all from Nikon Corp. (Tokyo, Japan).

Metabolic Labeling of CHL1 with Fatty Acids—One-day-old cultured cortical neurons maintained in wells of a 6-well culture plate were incubated with Click-iT® myristic acid or Click-iT® palmitic acid azide (Invitrogen) applied in the culture medium for 4.5 h. Neurons were then incubated for 15 min either with control nonimmune rabbit immunoglobulins or antibodies against the extracellular domain of CHL1 applied in the culture medium, washed two times with ice-cold PBS, lysed in 200 μl of lysis buffer (1% SDS, 50 mM Tris, pH 8.0), and stored at −80 °C. Myristic and palmitic acids incorporated into CHL1 were then labeled with biotin-alkyne using Click-iT® protein reaction buffer kit (Invitrogen) according to the manufacturer's instructions. CHL1 was then immunoprecipitated as described above (see under "Co-immunoprecipitation"). Mock immunoprecipitation with nonimmune immunoglobulins served as control. Immunoprecipitates were subjected to Western blot analysis.

Internalization of CHL1 from the Cell Surface as Measured by CHL1 Antibody Uptake—Antibody uptake in cultured hippocampal neurons was analyzed essentially as described (26). Neurons were analyzed 24 h after plating. When indicated, neurons were preincubated with methyl-β-cyclodextrin (5 mM, 15 min) (18), mevastatin (10 μM, 24 h) (27), nifedipine (10 μM, 15 min) (22), and pimozide (5 μM, 15 min) (22). In experiments with transfected neurons, neurons were transfected before plating using a Neon transfection system (Invitrogen) according to the manufacturer's instructions. Neurons were incubated for 1 h in a CO_2 incubator with goat polyclonal antibodies recognizing the extracellular domain of CHL1 or control nonimmune goat immunoglobulins. Neurons were then fixed with 4% formaldehyde in PBS, washed with PBS, blocked with 1% bovine serum albumin in PBS, and labeled with Cy2-conjugated donkey anti-goat antibodies for 30 min at room temperature to visualize surface-expressed CHL1-CHL1 antibody complexes. Following washing with PBS, neurons were post-fixed with 2% formaldehyde in PBS, permeabilized with 0.25% Triton X-100 in PBS, blocked with 1% BSA in PBS, and labeled with Cy3-conjugated donkey anti-goat antibodies for 30 min at room temperature to visualize surface and internalized CHL1-CHL1 antibody complexes. Images of labeled neurons were acquired with the Nikon C1si confocal microscope using NIS Elements software and an Oil Plan Apo VC ×60 objective (numerical aperture 1.4) (Nikon, Tokyo, Japan). Numbers of cell surface (Cy2- and Cy3-positive) and internalized (Cy3-positive Cy2-negative) CHL1 clusters (N_{surf} and N_{intern}, respectively) were counted using ImageJ software. Internalization rate was estimated as a ratio of $N_{intern}/(N_{intern} + N_{surf}) \times 100\%$. In control experiments, when nonimmune goat immunoglobulins were used instead of CHL1 antibodies, no Cy3 or Cy2 labeling was observed (data not shown) indicating that nonspecific binding and uptake of secondary antibodies were negligible. Analysis of the transferrin receptor uptake was performed using the protocol used for CHL1 antibodies but with respective primary and secondary antibodies.

RESULTS

CHL1 Is Palmitoylated in Response to Ligand Binding—The intracellular domain of mouse CHL1 contains a cysteine residue at position 1102 (Cys-1101 in human CHL1) located in the vicinity of the plasma membrane (Fig. 1*A*). We have described that cysteine residues in the intracellular domain of the neural cell adhesion molecule (NCAM) are palmitoylated, and this palmitoylation leads to the targeting of NCAM to lipid rafts and contributes to signaling events following activation of NCAM at the cell surface (28). Hence, we investigated whether CHL1 would also be palmitoylated. Cultures of cortical neurons were incubated with palmitic acid labeled with Click-iT tag. Because ligand binding, either by homophilic interaction or by function triggering antibodies, plays a role in palmitoylation of NCAM (22, 29), nonstimulated neurons were compared with neurons treated with function triggering CHL1 antibodies. Western blot analysis of CHL1 immunoprecipitates from these neurons showed that palmitic acid was incorporated into CHL1 with the higher labeling intensity observed for CHL1 antibody-treated neurons compared with neurons treated with nonimmune

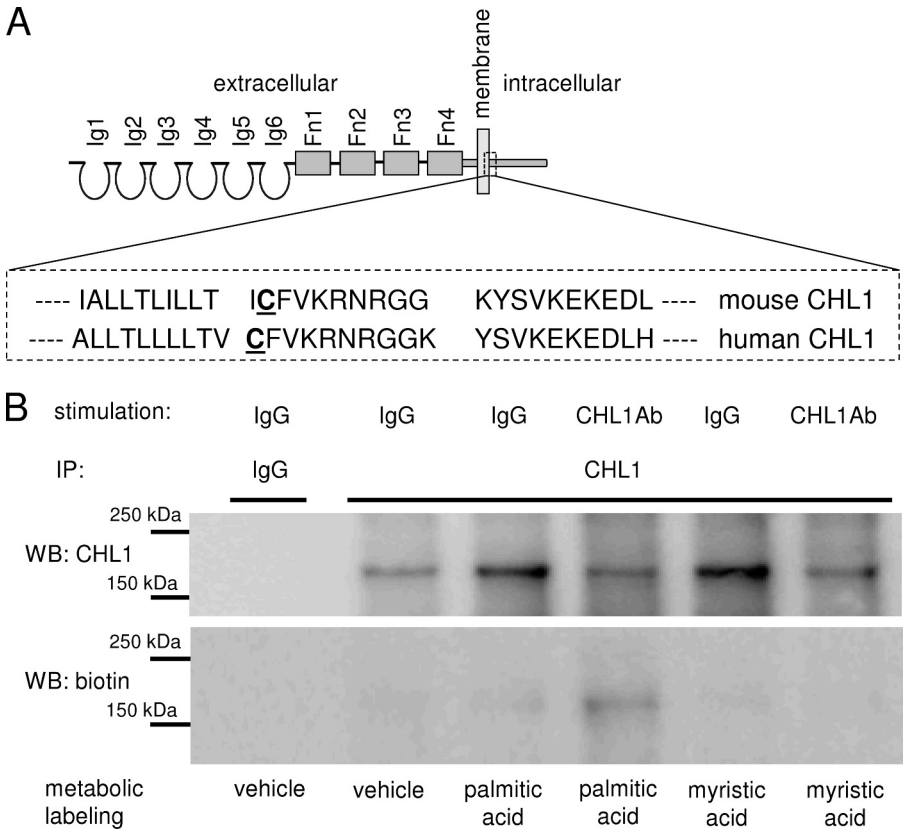

FIGURE 1. **CHL1 is palmitoylated.** *A,* schematic diagram of the structure of CHL1. Amino acid sequence (amino acids 1091–1130) of the membrane-proximal part of the intracellular domain CHL1 is shown in the *boxed inset*. Cysteine 1102 (mouse sequence) and cysteine 1101 (human sequence) are *underlined*. *Ig*, immunoglobulin-like domain; *Fn*, fibronectin type 3 repeat. *B,* cultured cortical neurons were metabolically labeled with palmitic and myristic acids or mock-treated with DMSO used to dilute the fatty acids. Neurons were stimulated by incubation with CHL1 antibodies or control nonimmune immunoglobulins (*IgG*). Incorporation of the fatty acids into CHL1 was analyzed by probing the CHL1 immunoprecipitates (*IP*) from cell lysates by Western blotting (*WB*) with HRP-avidin to detect biotin label incorporated into fatty acids by the Click-IT reaction.

immunoglobulins (Fig. 1*B*). In contrast, no labeling was found in neurons treated with myristic acid or neurons not treated with fatty acids, indicating that CHL1 specifically incorporates palmitic acid.

Cysteine 1102-dependent Targeting of CHL1 to Lipid Rafts Promotes the Association of βII Spectrin with Lipid Rafts—Palmitoylation is known to promote targeting of adhesion molecules to lipid rafts (28). To analyze whether CHL1 is present in lipid rafts, the total membrane fractions from brains of $CHL1^{+/+}$ and $CHL1^{-/-}$ mice were extracted with 1% Triton X-100 and used to isolate lipid rafts by flotation in a sucrose density gradient (18). Western blot analysis of these fractions showed that they were highly enriched in lipid raft markers, including Src family tyrosine kinase $p59^{Fyn}$ and glycosylphosphatidylinositol-anchored adhesion molecule contactin (Fig. 2*A*), indicating the efficiency of isolation. Lipid rafts from $CHL1^{+/+}$ but not $CHL1^{-/-}$ brains were also positive for CHL1 (Fig. 2*A*), confirming that CHL1 can associate with lipid rafts. By comparing enrichment of CHL1 in lipid rafts *versus* brain homogenates with that of lipid raft-localized contactin-1, we estimate that ~3% of all CHL1 molecules are localized to lipid rafts. This estimation is consistent with previous estimations of the lipid raft levels of NCAM, which is also targeted to lipid rafts by palmitoylation of its intracellular domain (28).

Because we had found that targeting of NCAM to lipid rafts was important for accumulating the NCAM-associated cytoskeleton in lipid rafts (18), we analyzed whether cytoskeletal proteins, which are associated with CHL1, would also be detectable in lipid rafts. The initial focus was centered on ankyrin-B, because ankyrins are binding partners for CHL1 (3). Based on the observations that ankyrins interact with spectrins (30) and that βII spectrin accumulates in axons, where CHL1 also accumulates (14), the levels of βII spectrin in lipid rafts were also analyzed. Both proteins were detected in lipid raft fractions by Western blot analysis (Fig. 2*A*) with ~30% of all βII spectrin and 20% of ankyrin-B estimated to be localized to lipid rafts.

Levels of ankyrin-B were increased by ~50% in lipid rafts from $CHL1^{-/-}$ brains compared with wild type ($CHL1^{+/+}$) brains (Fig. 2*A*). This increase is most likely due to the overall increased expression of ankyrin-B, which was increased by $106.7 \pm 35.8\%$ ($n = 4$, $p < 0.05$, paired *t* test) in $CHL1^{-/-}$ *versus* $CHL1^{+/+}$ brains. In contrast to ankyrin-B, the levels of βII spectrin were reduced by ~35% in $CHL1^{-/-}$ *versus* $CHL1^{+/+}$ lipid rafts (Fig. 2*A*), suggesting that CHL1 plays a role in targeting of βII spectrin to lipid rafts.

In agreement, levels of βII spectrin were ~5 times higher in lipid rafts from NIH 3T3 cells stably transfected with nonmutated wild type CHL1 (CHL1WT) when compared with nontransfected cells (Fig. 2*B*). To investigate whether cysteine 1102 plays a role in the association of CHL1 with lipid rafts, cysteine 1102 was mutated to serine by site-directed mutagenesis.

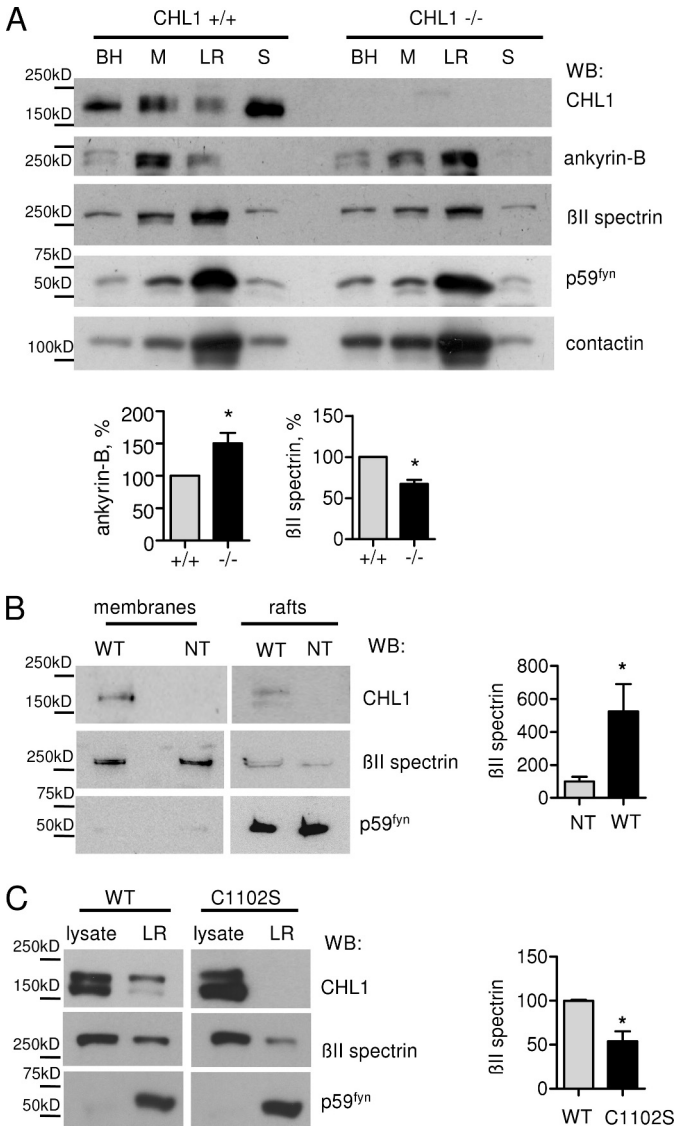

FIGURE 2. **CHL1 promotes targeting of βII spectrin to lipid rafts.** *A,* brain homogenate (*BH*), membrane fraction (*M*), lipid raft fraction (*LR*), and soluble fraction (*S*) from CHL1$^{+/+}$ and CHL1$^{-/-}$ brains were probed by Western blot analysis (*WB*) as indicated. Note that CHL1 is present in the lipid rafts. The soluble fraction contains CHL1 released from the plasma membrane by proteolytic cleavage of the extracellular domain. Note that the levels of βII spectrin are reduced, whereas levels of ankyrin-B are increased in lipid rafts from CHL1$^{-/-}$ *versus* CHL1$^{+/+}$ mice. Labeling for the lipid raft markers p59^{Fyn} and contactin-1 was performed to check the efficiency of lipid raft isolation. Representative blots are shown. *Graphs* represent the quantification of blots (mean values ± S.E., $n = 3$ experiments) with levels in CHL1$^{+/+}$ probes set to 100%. *, $p < 0.05$, paired *t* test. *B,* plasma membranes and lipid rafts were isolated from NIH 3T3 cells, which were either nontransfected (*NT*) or stably transfected with CHL1WT (*WT*), and probed by Western blotting (*WB*) as indicated. Note that levels of βII spectrin are higher in lipid rafts isolated from CHL1-transfected cells. *Graph* indicates the levels of βII spectrin in lipid rafts normalized to levels in nontransfected cells (mean values ± S.E., $n = 3$ experiments). *, $p < 0.05$, paired *t* test. *C,* lipid rafts were isolated from NIH 3T3 cells stably transfected with CHL1WT (*WT*) or CHL1C1102S (C1102S). Cell lysates (*lysate*) and lipid rafts (*LR*) were probed by Western blot analysis (*WB*) as indicated. Labeling for the lipid raft marker p59^{Fyn} was performed to check the efficiency of lipid raft isolation. Note that CHL1C1102S is not detectable in lipid rafts. Levels of βII spectrin are reduced in lipid rafts isolated from CHL1C1102S *versus* CHL1WT-transfected cells. *Graph* indicates the levels of βII spectrin in lipid rafts normalized to levels in CHL1WT probes (mean values ± S.E., $n = 3$ experiments). *, $p < 0.05$, paired *t* test.

CHL1WT and the CHL1C1102S mutant were stably transfected into NIH 3T3 cells that were then used for lipid raft isolation. Western blot analysis of lipid rafts from the transfected cells showed that levels of the lipid raft marker protein p59^{Fyn} were similar in lipid rafts isolated from both cell lines (Fig. 2*C*), indicating similar efficiencies of lipid raft isolation. However, although expression levels of CHL1C1102S analyzed in total cell lysates were similar to that of CHL1WT (Fig. 2*C*), only CHL1WT but not CHL1C1102S was detectable in lipid rafts (Fig. 2*C*), indicating that cysteine 1102 is critical for targeting of CHL1 to lipid rafts. Levels of βII spectrin were lower in lipid rafts isolated from CHL1C1102S-transfected cells when compared with cells transfected with CHL1WT (Fig. 2*C*) further suggesting a functional relationship between CHL1 and βII spectrin in lipid rafts.

CHL1 Forms a Complex with βII Spectrin—To investigate the relationship between CHL1 and βII spectrin, double immunofluorescence labeling of cultured 1-day-old hippocampal neurons with antibodies against CHL1 and βII spectrin was performed. CHL1 and βII spectrin were found to be co-expressed along neurites and in growth cones and somata of neurons (Fig. 3*A*). The distribution of CHL1 and βII spectrin in these cells overlapped partially. Clusters of CHL1 in growth cones often co-localized with βII spectrin accumulations, being particularly evident in large growth cones (Fig. 3, *A* and *C*). Clustering of CHL1 at the neuronal cell surface induced by application of CHL1 antibodies to live neurons resulted in partial redistribution of βII spectrin to CHL1 clusters and increased co-localization of CHL1 and βII spectrin (Fig. 3, *B* and *C*; coefficient of correlation between distributions of CHL1 and βII spectrin in neurons treated with CHL1 antibodies is 0.82 ± 0.01 ($n = 25$ neurons were analyzed); coefficient of correlation between distributions of CHL1 and βII spectrin in neurons treated with nonspecific immunoglobulins is 0.37 ± 0.03 ($n = 27$ neurons were analyzed)).

To investigate the possibility that CHL1 and βII spectrin engage in direct interactions, a proximity ligation assay was performed to analyze whether βII spectrin and the intracellular domain of CHL1 can be in close proximity (<40 nm), with this dimension being characteristic of complex formation. In cultured hippocampal neurons, the proximity ligation assay with antibodies against βII spectrin and the intracellular domain of CHL1 produced a positive reaction (Fig. 3*D*). CHL1-βII spectrin complexes revealed by this assay were seen along neurites and in growth cones (Fig. 3*D*). Omission of CHL1 antibodies (Fig. 3*D*, *control*) or βII spectrin antibodies (data not shown) completely eliminated the signal, indicating the specificity of the reaction.

To analyze whether CHL1 forms a complex with βII spectrin in the intact tissue, co-immunoprecipitation experiments were performed using brain homogenates, which showed that βII spectrin co-immunoprecipitated with CHL1 from lysates of brains of 1–3-day-old mice (Fig. 3*E*). In contrast, βI spectrin, a dendritic spectrin isoform, was not detected in the CHL1 co-immunoprecipitates (Fig. 3*E*).

To investigate whether CHL1 and βII spectrin can interact directly, spectrin purified from mouse brain (Fig. 3*F*) was immobilized in wells of a 96-well plate substrate-coated with

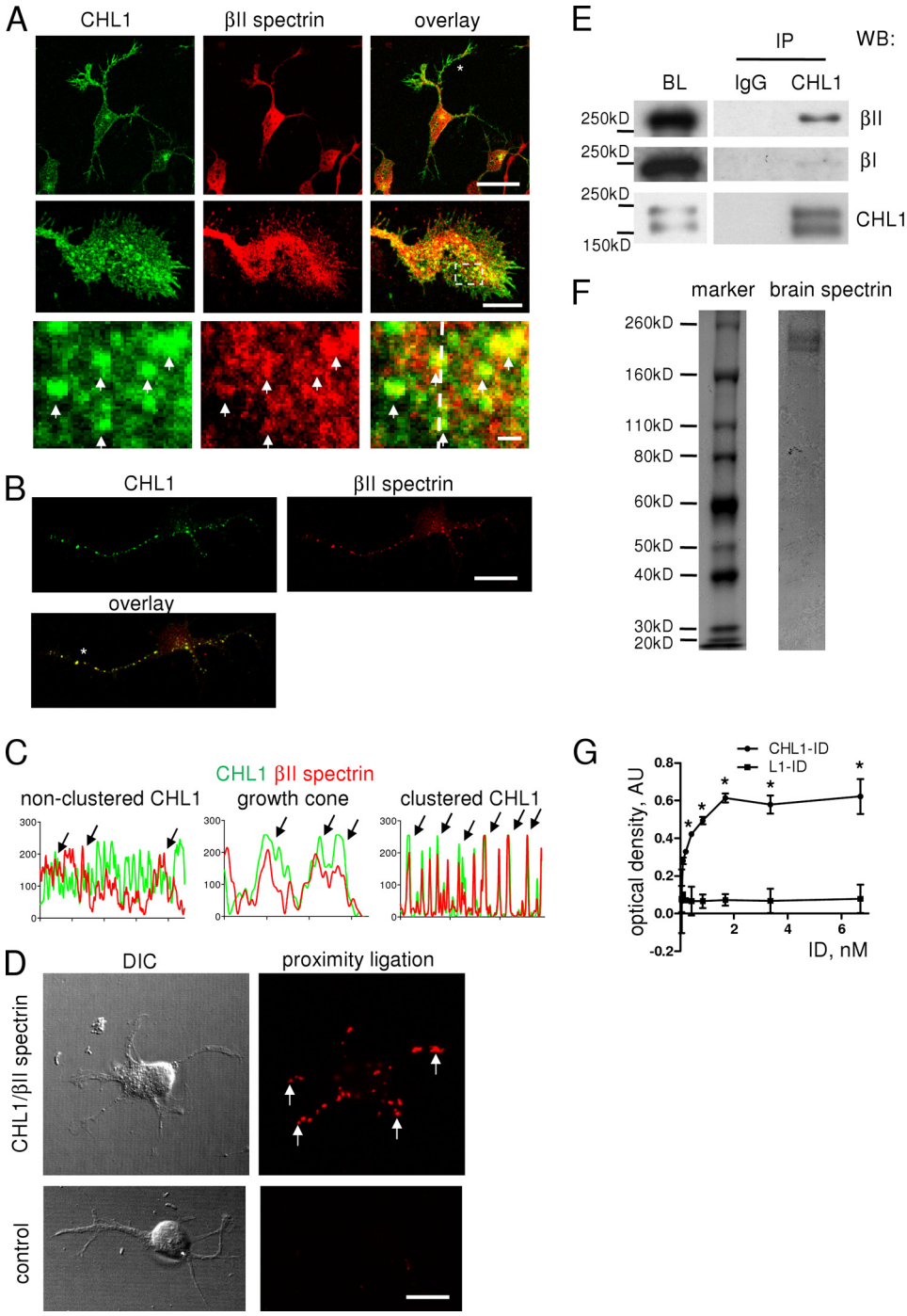

FIGURE 3. **CHL1 associates with βII spectrin.** *A,* cultured hippocampal neurons co-labeled by indirect immunofluorescence for CHL1 and βII spectrin are shown. High magnification images (*lower panels*) show a growth cone and enlarged image of the area marked by *dashed lines* in the *overlay*. CHL1 and βII spectrin partially co-localize along neurites and in growth cones. *Arrows* indicate clusters of CHL1 overlapping with βII spectrin accumulations. *Scale bars,* 20 μm (*upper panel*), 10 μm (*middle panel*), and 1 μm (*lower panel*). *B,* CHL1 was clustered at the cell surface of live hippocampal neurons in culture. Neurons were then fixed and co-labeled with antibodies against βII spectrin. Note that clusters of CHL1 co-localize with βII spectrin accumulations. *Scale bar,* 20 μm. *C,* profiles of CHL1 and βII spectrin immunofluorescence labeling intensities measured along neurites marked with *asterisks* in *A* and *B* and along a *dashed line* in growth cone in *A*. *Arrows* indicate overlapping peaks in distributions of both proteins. *D,* proximity ligation assay with antibodies against βII spectrin and the intracellular domain of CHL1 (*left panel*). *Arrows* show examples of putative CHL1-βII spectrin complexes in growth cones. A proximity ligation reaction without CHL1 antibodies served as control (*right panel*). *DIC,* differential interference contrast images. *Scale bar,* 20 μm. *E,* CHL1 was immunoprecipitated (*IP*) from brain lysates from 1- to 3-day-old mice. Mock immunoprecipitation with nonimmune rabbit immunoglobulin (*IgG*) was performed as a control. Brain lysates (*BL*, ~10% of input) and immunoprecipitates were analyzed by Western blotting (*WB*) as indicated. Note that βII spectrin but not βI spectrin co-immunoprecipitated with CHL1. *F,* gel shows purified brain spectrin used for the *in vitro* protein binding assay (*G*). *G,* βII spectrin was immobilized in wells of a 96-well plate and assayed for its ability to bind increasing concentrations of the intracellular domain (*ID*) of CHL1-ID or L1 (*L1-ID*). The experiment was performed three times with the same results. Mean values (A_{405}) ± S.E. for a representative experiment carried out in triplicate are shown. *, $p < 0.001$, repeated measures ANOVA with Tukey's multiple comparison test. *AU,* arbitrary units.

βII spectrin antibody, and its ability to capture the recombinant intracellular domain (ID) of CHL1 was analyzed. CHL1-ID bound to βII spectrin in a concentration-dependent manner (Fig. 3*G*), whereas L1-ID analyzed for comparison did not interact with βII spectrin (Fig. 3*G*).

Ligand-induced Clustering of CHL1 Induces Partial Removal of Spectrin from the Plasma Membrane and Internalization of CHL1 in a Lipid Raft-dependent Manner—Lipid rafts are often considered as sites of cytoskeleton remodeling (31), and abnormal levels of βII spectrin and ankyrin-B in lipid rafts may reflect abnormal spectrin meshwork restructuring. To investigate this idea, we examined the impact of CHL1 deficiency on the detergent insolubility of βII spectrin and ankyrin-B, which is a measure of their incorporation level into the detergent-resistant submembrane cytoskeleton (18). $CHL1^{+/+}$ and $CHL1^{-/-}$ brain homogenates were extracted with 0.1% Triton X-100 to obtain 0.1% Triton X-100-insoluble and -soluble fractions, which were then analyzed by Western blot. This analysis showed that overall levels of 0.1% Triton X-100-insoluble βII spectrin and ankyrin-B were increased in $CHL1^{-/-}$ brains (Fig. 4). Not only the overall levels of 0.1% Triton-insoluble βII spectrin were increased but also the percentage of 0.1% Triton-insoluble βII spectrin relative to its total levels was higher in $CHL1^{-/-}$ brains (87.1 ± 2.3 and 93.5 ± 2.3% of total brain βII spectrin were insoluble, whereas 12.8 ± 2.3 and 6.5 ± 0.3% of βII spectrin were soluble in 0.1% Triton X-100 in $CHL1^{+/+}$ and $CHL1^{-/-}$ brains, respectively ($n = 3$, $p < 0.05$, paired *t* test)). Interestingly, the percentage of soluble ankyrin-B was increased in $CHL1^{-/-}$ *versus* $CHL1^{+/+}$ brains (2.5 ± 0.3 and 4.6 ± 0.4% of ankyrin-B were soluble, and 95.4 ± 0.3 and 97.4 ± 0.4% were insoluble in 0.1% Triton X-100 in $CHL1^{+/+}$ and $CHL1^{-/-}$ brains, respectively ($n = 3$, $p < 0.05$, paired *t* test)). Saturation of the binding sites for other ankyrin-B binding partners at the plasma membrane due to the overall increased expression of ankyrin-B in $CHL1^{-/-}$ mice could be a factor contributing to an increase in the percentage of soluble ankyrin-B in $CHL1^{-/-}$ mice.

Polymerized spectrins form a meshwork beneath the plasma membrane. Because CHL1 deficiency increased levels of polymerized spectrin cytoskeleton, we analyzed whether ligand binding by CHL1 influences the association of βII spectrin with the plasma membrane. NIH 3T3 cells transfected with CHL1WT or the CHL1C1102S mutant were treated with CHL1 antibodies applied in the culture medium. To analyze levels of βII spectrin attached to the cytoplasmic leaflet of the plasma membrane by interaction with transmembrane proteins, cell surface-exposed proteins in transfected 3T3 cells were biotinylated and separated from the total protein pool. The levels of βII spectrin that co-purified with the cell surface proteins were then analyzed by Western blot. This analysis showed that after application of CHL1 antibodies to CHL1WT-transfected cells, the amount of surface membrane-associated βII spectrin decreased by ~50% (Fig. 5*A*). In contrast, levels of membrane-associated clathrin (Fig. 5*A*) or Na^+/K^+-ATPase (data not shown) did not significantly change after CHL1 antibody application.

CHL1 antibody-induced detachment of βII spectrin from the cell surface plasma membrane was blocked in CHL1C1102S-transfected cells, indicating that lipid raft localization of CHL1 is necessary for this effect (Fig. 5*A*). Interestingly, we also found that application of CHL1 antibodies resulted in an ~40% decrease in the levels of CHL1WT at the cell surface (Fig. 5*A*). This effect was also blocked in CHL1C1102S-transfected cells (Fig. 5*A*). The total levels of full-length CHL1WT were not changed in CHL1 antibody-treated cells (Fig. 5*B*), excluding possible shedding of CHL1WT from the cell surface and suggesting that CHL1 antibody treatment induced internalization of CHL1WT but not CHL1C1102S.

The role of lipid rafts in CHL1 endocytosis was then assessed in cultured hippocampal neurons by means of fluorescence microscopy by analyzing cell surface-bound CHL1 antibody uptake as a measure of CHL1 endocytosis (26). Lipid rafts were disrupted by preincubating neurons for 24 h with mevastatin, which is an inhibitor of cholesterol synthesis and lipid raft assembly. Alternatively, neurons were incubated for 15 min with methyl-β-cyclodextrin, which disintegrates lipid rafts.

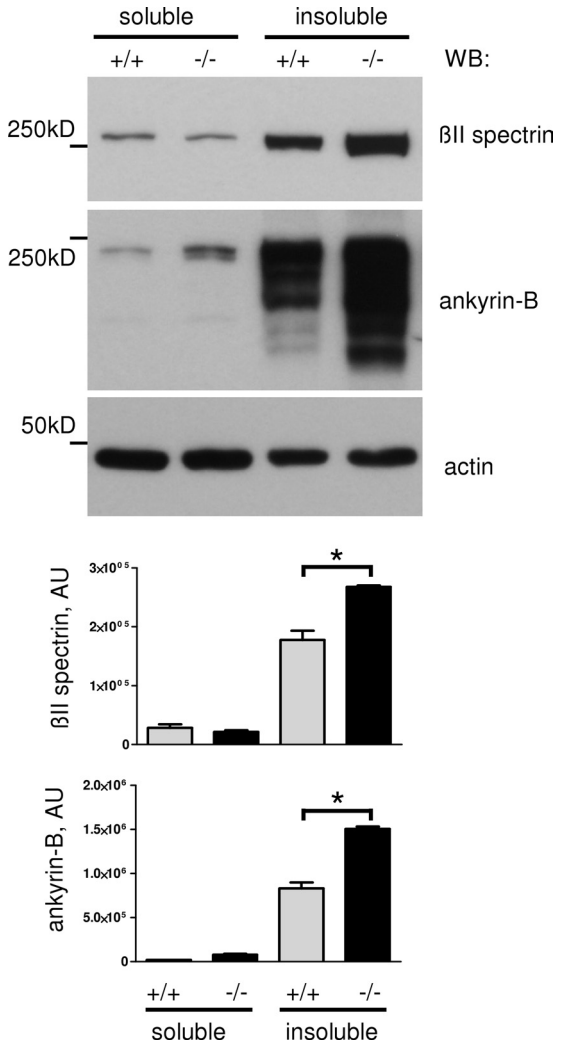

FIGURE 4. **Spectrin meshwork polymerization is increased in $CHL1^{-/-}$ brains.** $CHL1^{+/+}$ and $CHL1^{-/-}$ brain homogenates were extracted with 0.1% Triton X-100. Detergent-soluble and -insoluble fractions were analyzed by Western blotting (*WB*) as indicated. Note that levels of detergent-insoluble βII spectrin and ankyrin-B are increased in $CHL1^{-/-}$ brains. *Graph* represents the quantification of the blots (mean values ± S.E., $n = 3$ experiments; *AU,* arbitrary units). *, $p < 0.05$, paired *t* test.

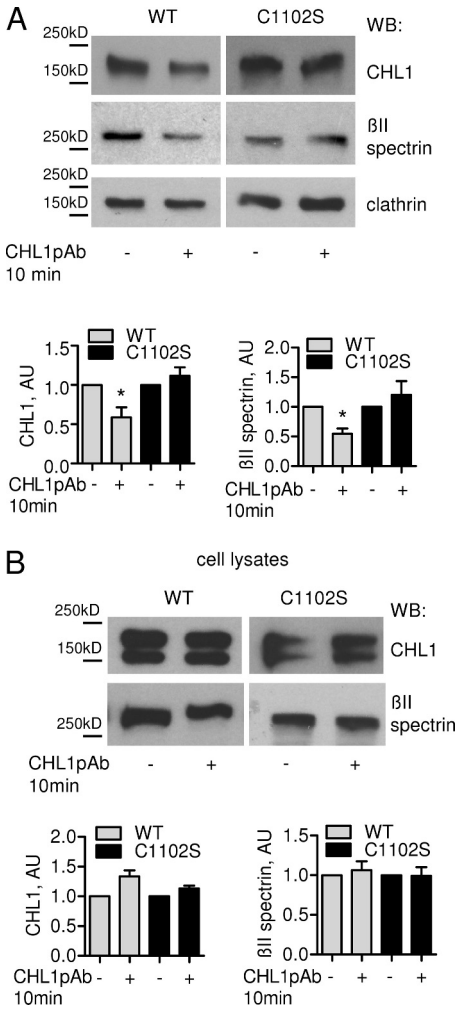

FIGURE 5. **CHL1 antibody treatment induces detachment of βII spectrin from the cell surface.** *A,* live NIH 3T3 cells transfected with CHL1WT or CHL1C1102S were treated with CHL1 polyclonal antibodies for 10 min. Cell surface proteins were then biotinylated and precipitated with neutravidin-coupled agarose beads after the cell lysis. Precipitates were analyzed by Western blotting (*WB*) as indicated. Note that levels of CHL1 and cell surface protein-associated βII spectrin are reduced in CHL1WT but not in CHL1C1102S-transfected cells treated with CHL1 antibodies. Levels of clathrin are not affected. *B,* total levels of CHL1 and βII spectrin are similar in cell lysates of CHL1WT and CHL1C1102S-transfected cells either treated or not treated with CHL1 antibodies. *A* and *B*, *graphs* represent quantification of blots with signals in control cells set to 1 (mean values ± S.E., $n = 3$ experiments). *, $p < 0.05$, paired *t* test. *AU,* arbitrary units.

Neurons were then incubated with CHL1 antibodies applied for 60 min. Following fixation with paraformaldehyde, surface and total pools of CHL1 antibody-CHL1 complexes were visualized using green and red fluorochrome-coupled secondary antibodies applied before and after permeabilization of neurons with detergent, respectively. Fluorescence microscopic analysis showed that application of CHL1 antibodies resulted in clustering of CHL1 along neurites and in somata (Fig. 6*A*). Approximately 15 and 30% of CHL1 clusters in neurites and soma, respectively, were positive only for the red fluorochrome, which was applied after permeabilization with detergent (Fig. 6*A*). These clusters were thus identified as internalized CHL1. The number of internalized clusters of CHL1 was reduced in neurons treated with methyl-β-cyclodextrin or mevastatin (Fig. 6*A*) indicating that lipid raft integrity is required for CHL1 endocytosis. In contrast, methyl-β-cyclodextrin or mevastatin did not affect internalization of transferrin receptors as measured by analyzing the uptake of antibodies against these receptors (Fig. 6*A*). Internalization of CHL1 was also reduced in neurons transfected with the CHL1C1102S mutant when compared with neurons transfected with CHL1WT (Fig. 6*B*).

Ligand-induced Endocytosis of CHL1 Is Accompanied by CHL1-βII Complex Disruption and Depends on L-type VDCC—To investigate whether the CHL1-dependent detachment of βII spectrin from the plasma membrane correlates with the dissociation of the CHL1-βII spectrin complex, co-immunoprecipitation experiments were performed. CHL1WT and CHL1C1102S were immunoprecipitated from transfected 3T3 cells either treated or not treated with CHL1 antibodies. Levels of βII spectrin that co-immunoprecipitated with CHL1WT from CHL1 antibody-treated cells were reduced by ~50% when compared with control cells not treated with antibodies (Fig. 7*A*). In contrast, the association of CHL1C1102S with βII spectrin was not affected following CHL1 antibody application (Fig. 7*A*), indicating that the CHL1-βII spectrin complex disassembly is lipid raft-dependent.

In searching for the mechanisms of the CHL1-βII spectrin complex disassembly, we analyzed whether changes in Ca^{2+} concentration would influence the CHL1-βII spectrin complex. CHL1 was immunoprecipitated from brain lysates either in the presence of the Ca^{2+}-sequestering agent EGTA or in the presence of various concentrations of Ca^{2+}. The highest co-immunoprecipitation efficiency of βII spectrin with CHL1 was observed in the presence of EGTA, whereas the co-immunoprecipitation efficiency was reduced by ~50 and 80% when 0.2 mM Ca^{2+} and 2 mM Ca^{2+} were added to the brain lysates, respectively (Fig. 7*B*). Interestingly, the direct interaction between CHL1-ID and βII spectrin *in vitro* was not changed in the presence of 2 mM Ca^{2+} (data not shown), suggesting that Ca^{2+} induces the disruption of CHL1-βII spectrin complex indirectly.

T- and L-type VDCCs are present at high levels in lipid rafts (22). Thus, we used cell surface biotinylation to analyze whether Ca^{2+} influx via these channels plays a role in endocytosis of CHL1 by incubating CHL1WT-transfected 3T3 cells with CHL1 antibodies in the presence of nifedipine, an L-type VDCC inhibitor, and pimozide, a T-type VDCC inhibitor. Internalization of CHL1WT was significantly inhibited in cells incubated with nifedipine but not pimozide (Fig. 7*C*). The overall expression of CHL1WT was not altered by VDCC inhibitors as shown by Western blot analysis of total cell lysates (Fig. 7*D*). In contrast to CHL1, levels of cell surface-associated clathrin or Na^+/K^+-ATPase (data not shown) were not changed after CHL1 antibody application both in control and VDCC inhibitor-treated cells (Fig. 7*C*).

We then analyzed the effect of nifedipine on the association of CHL1 with lipid rafts in cultured hippocampal neurons. Because cultured neurons are not suitable for biochemical isolation of lipid rafts because of the large amount of material required for this protocol, lipid rafts were visualized *in situ* by extracting cultured neurons with cold 1% Triton X-100 and labeling with fluorescent cholera toxin, which binds to the lipid raft marker ganglioside GM1 (22). Application of CHL1 anti-

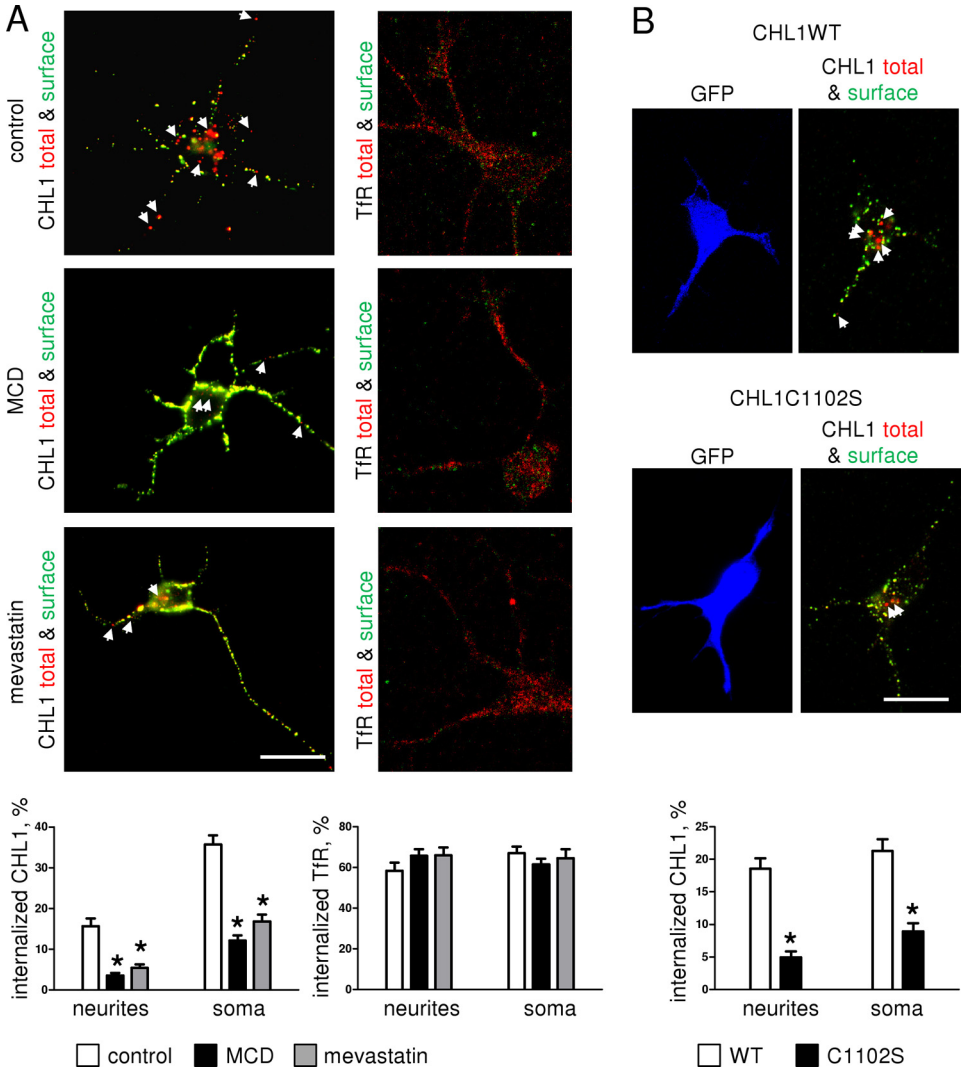

FIGURE 6. **Antibody-induced clustering of CHL1 at the cell surface induces its endocytosis in a lipid raft-dependent manner.** *A,* cultured live hippocampal neurons, either not treated (control) or pretreated with methyl-β-cyclodextrin (*MCD*) or mevastatin, were incubated with CHL1 or transferrin receptor (*TfR*) antibodies. After fixation, cell surface CHL1-antibody or TfR-antibody complexes were visualized using green fluorochrome before cell permeabilization, and total CHL1-antibody or TfR-antibody complexes were visualized using red fluorochrome after cell permeabilization with detergent. Note that CHL1 antibody induces clustering of CHL1 at the cell surface (*green/red* positive clusters seen as *yellow* accumulations). *Arrows* show accumulations of internalized CHL1 (*red* accumulations). Note that CHL1 internalization is inhibited by methyl-β-cyclodextrin and mevastatin, although internalization of TfR is not affected. *Graphs* represent percentage of internalized accumulations of CHL1 and TfR in somata and along neurites (mean values ± S.E., $n = 60$ neurons were analyzed in three independent experiments), *, $p < 0.05$, one-way ANOVA with Tukey's multiple comparison test, compared with control. *B,* CHL1 internalization was analyzed in cultured hippocampal neurons transfected with CHL1WT or CHL1C1102S. *Arrows* show accumulations of internalized CHL1. Note that CHL1 internalization is reduced in CHL1C1102S-transfected neurons. *Graph* represents percentage of internalized accumulations of CHL1 in somata and along neurites (mean values ± S.E., $n = 60$ neurons were analyzed in three independent experiments), *, $p < 0.05$, *t* test, compared with WT. *A* and *B*, *scale bars,* 20 μm.

bodies increased the numbers of detergent-insoluble clusters of CHL1, which co-localized with accumulations of βII spectrin (Fig. 8). Overall levels of detergent-insoluble CHL1 and βII spectrin and their levels measured in cholera toxin-positive accumulations were increased in neurons incubated with CHL1 antibodies when compared with neurons incubated with non-immune immunoglobulins (Fig. 8) indicating increased association with lipid rafts. Levels of CHL1 and βII spectrin in lipid rafts were further increased in neurons treated with CHL1 antibodies in the presence of nifedipine (Fig. 8), suggesting that Ca^{2+} influx via L-type VDCC negatively regulates levels of the CHL1-βII spectrin complexes in lipid rafts.

In agreement with biochemical data (Fig. 7), fluorescence microscopic analysis of cultured neurons showed that nifedipine but not pimoside inhibited internalization of CHL1 (Fig. 9*A*). To analyze whether a reduction in the association of CHL1 with βII spectrin would influence internalization of CHL1, neurons were transfected with βII spectrin siRNA. A reduction in βII spectrin expression in neurons transfected with functional βII spectrin siRNA correlated with increased endocytosis of CHL1 when compared with neurons transfected with control nonsilencing siRNA or nonfunctional βII spectrin siRNA (Fig. 9*B*).

Ca^{2+} Influx via VDCCs and Association of CHL1 with Lipid Rafts Is Required for CHL1-dependent Neurite Outgrowth—Next, we investigated whether CHL1 ligand-induced neurite outgrowth depends on VDCCs and lipid rafts. Cultured hippocampal $CHL1^{+/+}$ neurons were treated for 24 h with CHL1 anti-

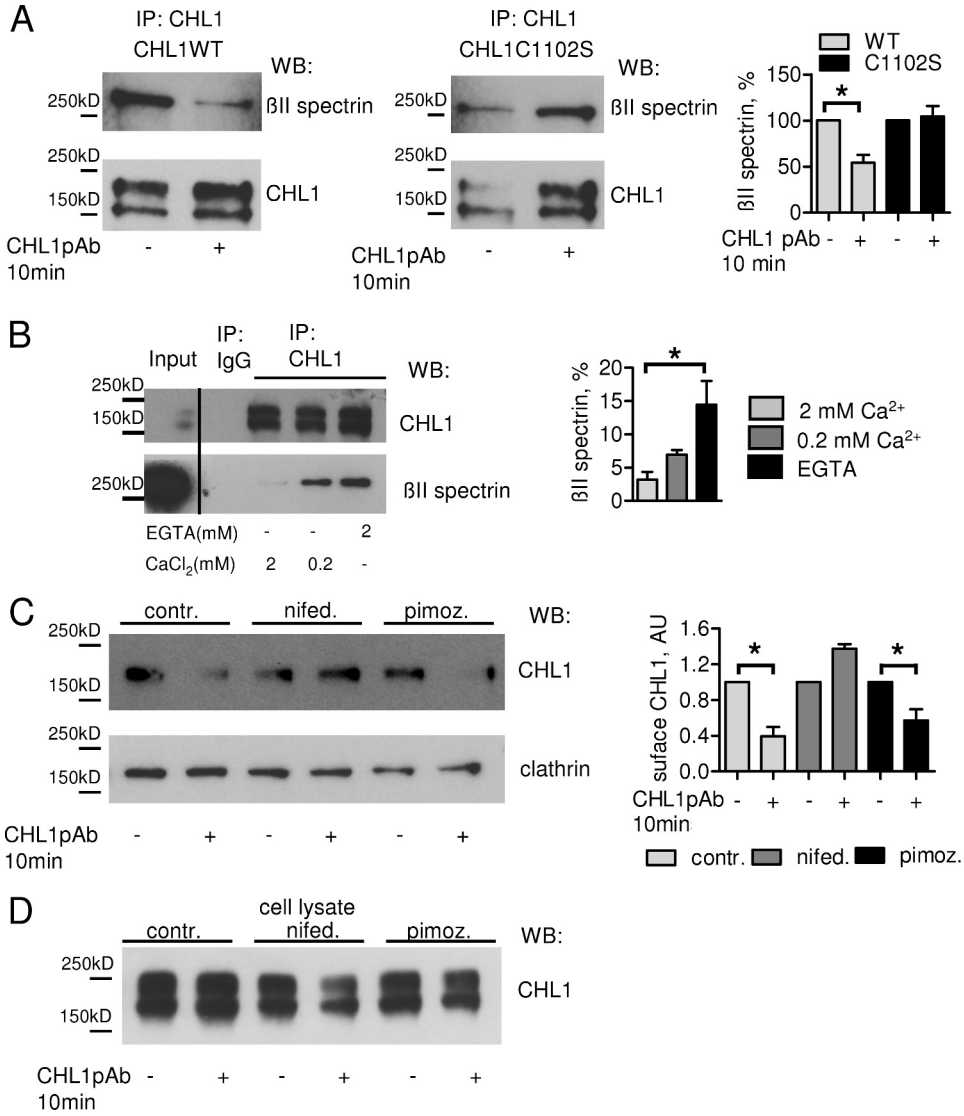

FIGURE 7. **CHL1-βII spectrin complex is disrupted in a Ca^{2+}-dependent manner.** *A,* CHL1 was immunoprecipitated (*IP*) from NIH 3T3 cells transfected with CHL1WT or CHL1C1102S that were either treated or not treated with CHL1 polyclonal antibodies for 10 min. Note that the co-immunoprecipitation of βII spectrin with CHL1 is reduced in CHL1 antibody-treated cells transfected with CHL1WT but not CHL1C1102S. *Graph* represents the quantification of the blots (mean values ± S.E., $n = 3$ experiments). The levels of the co-immunoprecipitated βII spectrin were normalized to the levels of the immunoprecipitated CHL1, and signals in cells not treated with CHL1 antibodies were set to 100%. *, $p < 0.05$, paired *t* test. *B,* CHL1 was immunoprecipitated from membrane fractions of $CHL1^{+/+}$ mice in the presence of 2 mM Ca^{2+}, 0.2 mM Ca^{2+}, or 2 mM EGTA. Total brain homogenate (*input* material) and precipitates were analyzed by Western blotting (*WB*) as indicated. Note that the co-immunoprecipitation of βII spectrin is inhibited in the presence of Ca^{2+}. *Graph* represents the quantification of blots (mean values ± S.E., $n = 3$ experiments). Levels of the co-immunoprecipitated βII spectrin were normalized to its total levels in the input material. *, $p < 0.05$, one-way ANOVA with Tukey's multiple comparison test. *C* and *D,* NIH 3T3 cells transfected with CHL1WT were treated with CHL1 antibodies in the presence or absence of the VDCC inhibitors nifedipine (*nifed.*) or pimozide (*pimoz.*). *contr,* control. Surface proteins were then biotinylated and precipitated from cell lysates with neutravidin-agarose beads. Lysates (*D*) and precipitates (*C*) were analyzed by Western blotting (*WB*) as indicated. Note that nifedipine, but not pimozide, inhibits CHL1 antibody-induced reduction of CHL1 levels at the cell surface. Clathrin was used as loading control. The overall CHL1 expression in cell lysates was not affected by CHL1 antibodies and VDCC inhibitors (*D*). *Graph* (*C*) represents the quantification of blots (mean values ± S.E., $n = 3$ experiments, signals in probes from cells not treated with CHL1 antibodies set to 1). *, $p < 0.05$, paired *t* test. *AU,* arbitrary units.

bodies or nonspecific control immunoglobulins applied in the culture medium either in the presence or absence of nifedipine, pimozide, and cholesterol or sphingolipid biosynthesis inhibitors, which inhibit lipid raft assembly. Analysis of the microscopic images of these neurons showed that neurons treated with CHL1 antibodies in the absence of inhibitors had ~30% longer putative axons, identified as longest neurites, when compared with control neurons incubated with nonspecific immunoglobulins (Fig. 10, *A* and *B*). CHL1 antibody treatment also increased the total neurite length of all neurites per neuron by ~85% (Fig. 10, *A* and *B*). This increase in neurite length was blocked by nifedipine (Fig. 10*A*), indicating that Ca^{2+} influx via L-type VDCCs is required for CHL1 ligand-induced neurite outgrowth. Surprisingly, pimozide also inhibited CHL1 ligand-induced neurite outgrowth (Fig. 10*A*), suggesting that although Ca^{2+} influx via T-type VDCCs is not required for ligand-induced endocytosis of CHL1, these channels are involved in other signaling events activated by CHL1. CHL1-dependent increase in neurite outgrowth was also inhibited by mevinolin, an inhibitor of cholesterol synthesis, the fungal metabolite fumonisin B that inhibits biosynthesis of sphingolipids, and NB-DNJ, a blocker of glycosphingolipid synthesis (Fig. 10*B*).

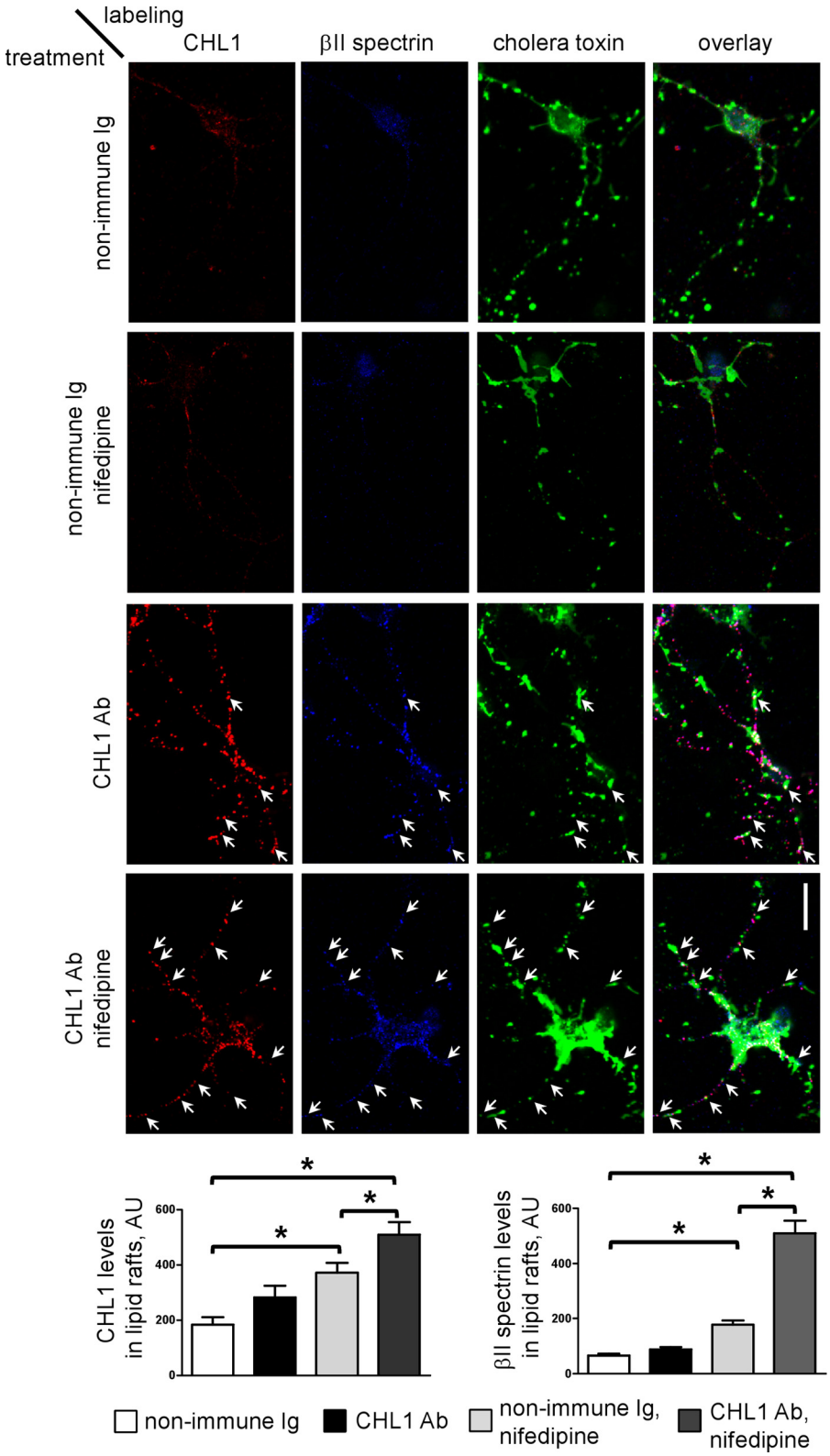

FIGURE 8. **Inhibition of L-type VDCC promotes CHL1 antibody-induced accumulation of CHL1 and βII spectrin in lipid rafts.** Cultured hippocampal neurons were incubated with nonimmune immunoglobulins (*Ig*) or CHL1 antibodies (*Ab*) either in the presence or absence of nifedipine. Neurons were then extracted in cold 1% Triton X-100 and co-labeled with fluorescent cholera toxin and indirect immunofluorescence against CHL1 and βII spectrin. *Arrows* indicate CHL1-βII spectrin clusters overlapping with cholera toxin-labeled GM1 accumulations. Note higher co-localization of CHL1-βII spectrin complexes with GM1 clusters in nifedipine-treated neurons. *Scale bar*, 20 μm. *Graphs* show mean levels ± S.E. of CHL1 and βII spectrin labeling intensities in GM1 clusters ($n = 50$ neurons were analyzed in three independent experiments). *, $p < 0.05$, ANOVA with Newman-Keuls multiple comparison test. *AU*, arbitrary units.

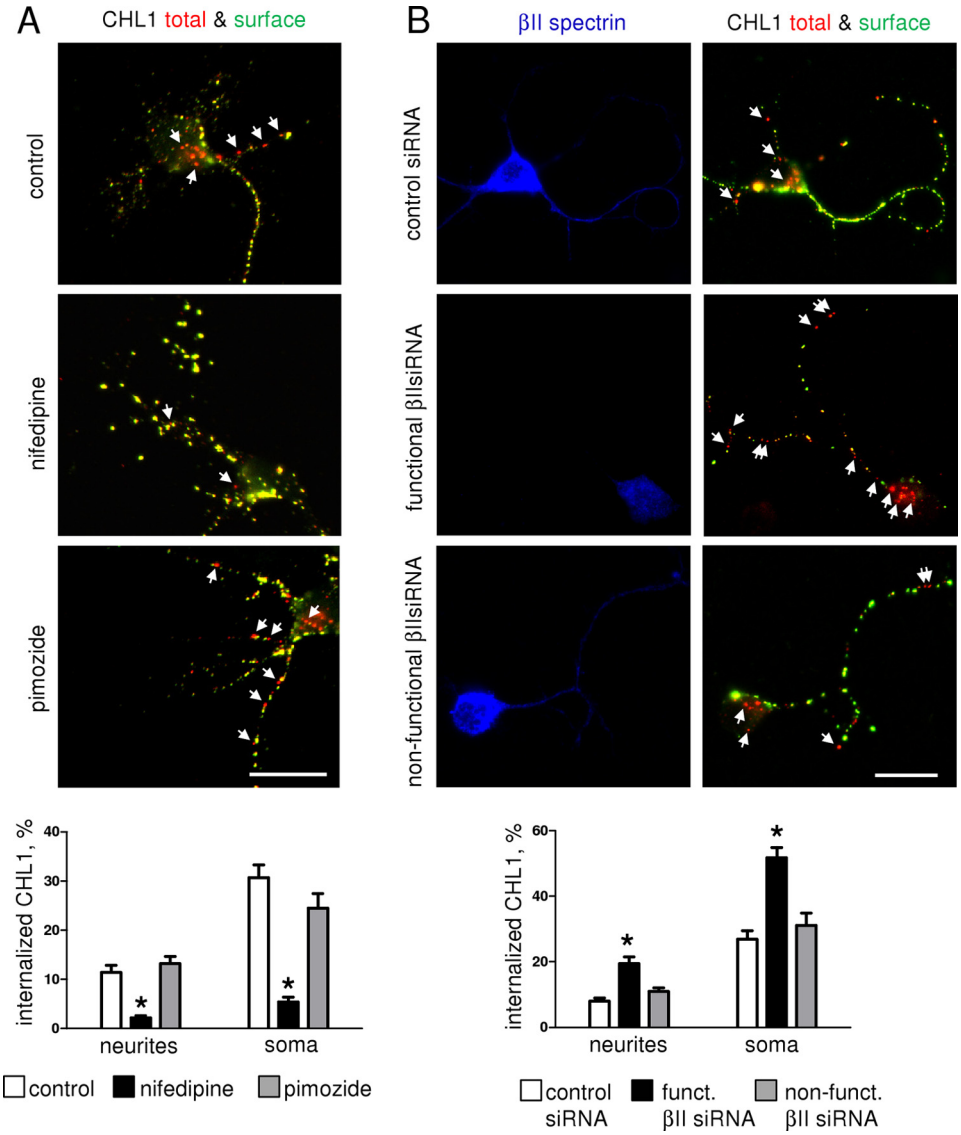

FIGURE 9. **Antibody-induced endocytosis of CHL1 is blocked by nifedipine and enhanced by βII spectrin expression knockdown.** *A,* CHL1 antibody uptake was analyzed in neurons either not treated (*control*) or pretreated with nifedipine or pimoside. *Arrows* show *red* accumulations of internalized CHL1. Note that CHL1 internalization is inhibited by nifedipine. *B,* CHL1 antibody uptake was analyzed in neurons transfected with control siRNA and functional or nonfunctional βII spectrin siRNA. *Arrows* show *red* accumulations of internalized CHL1. Neurons were co-labeled with antibodies against βII spectrin. Note lower levels of βII spectrin along neurites and in soma and higher endocytosis of CHL1 in the neuron transfected with functional βII spectrin siRNA. *A* and *B*, *graphs* represent percentage of internalized accumulations of CHL1 in somata and along neurites (mean values ± S.E., $n = 60$ neurons were analyzed in three independent experiments), *, $p < 0.05$, one-way ANOVA with Tukey's multiple comparison test, compared with all other groups. *Scale bar,* 20 μm.

These inhibitors did not affect neurite outgrowth in neurons incubated with control nonimmune immunoglobulins (Fig. 10*B*).

We then asked whether targeting of CHL1 to lipid rafts is required for CHL1 ligand-induced neurite outgrowth. Cultured $CHL1^{+/+}$ hippocampal neurons were transfected with the fluorescent protein cherry alone or cherry together with CHL1WT or CHL1C1102S. Exposure of cherry-only transfected neurons to CHL1 antibodies applied in the culture medium resulted in an ~30% increase in the length of longest neurites and 90% increase in total neurite length per neuron when compared with nonspecific immunoglobulin-treated cherry-transfected neurons (Fig. 10*C*). The basal neurite outgrowth in neurons co-transfected with cherry together with CHL1WT was reduced when compared with cherry-only transfected neurons (Fig. 10*C*). This observation is in agreement with our previous data showing that increased CHL1-mediated homophilic adhesion inhibits neurite outgrowth (2). Application of CHL1 antibodies to CHL1WT/cherry co-transfected neurons elicited an increase in neurite length that was similar to that in cherry-only transfected neurons (Fig. 10*C*). In contrast, the response to CHL1 antibodies was inhibited in neurons co-transfected with cherry and CHL1C1102S (Fig. 10*C*), suggesting that CHL1C1102S, which is not endocytosed in response to antibody application (Figs. 5 and 6*B*), interfered with neurite outgrowth.

DISCUSSION

Previous studies indicated that CHL1 plays a dual role in the developing nervous system by both promoting neurite out-

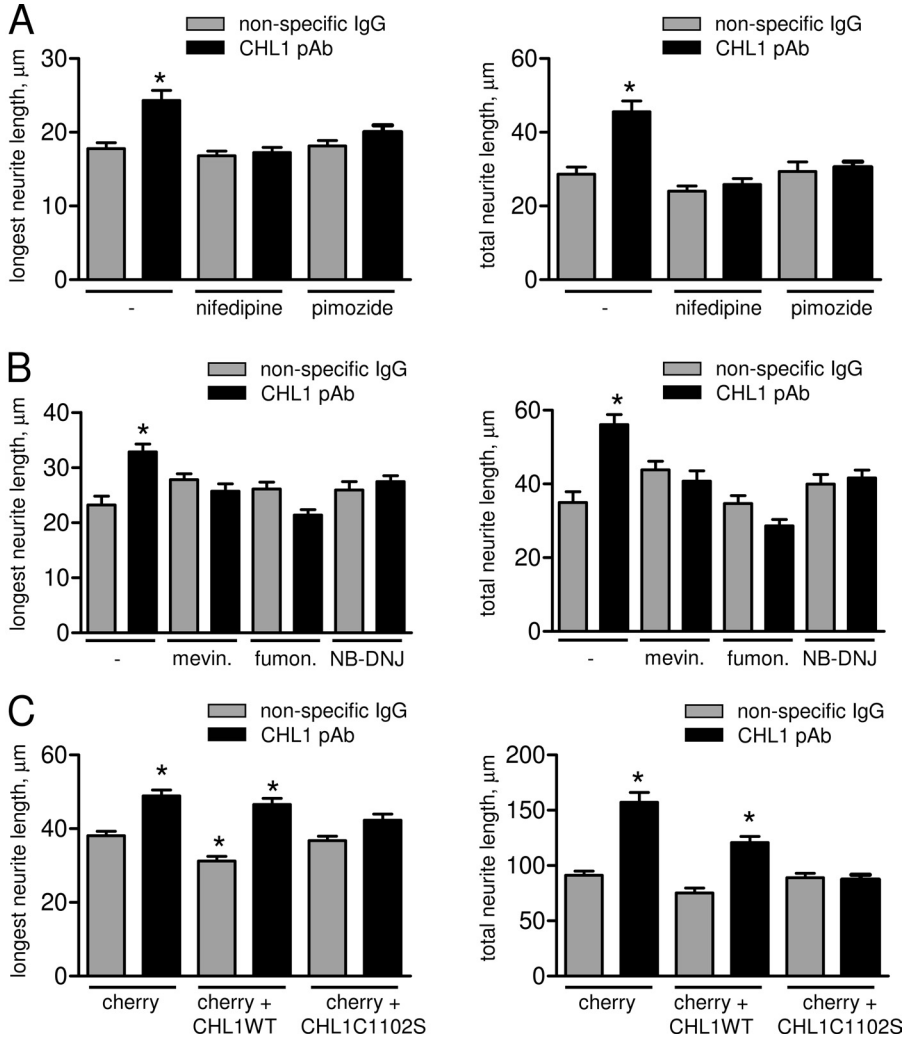

FIGURE 10. **CHL1 ligand-induced neurite outgrowth depends on the association of CHL1 with lipid rafts and Ca^{2+} influx via VDCCs.** *A* and *B,* cultured hippocampal neurons were treated for 24 h with nonspecific immunoglobulins (*IgG*) or CHL1 antibodies (*CHL1 pAb*) in the presence or absence of L- and T-type VDCC inhibitors nifedipine and pimozide (*A*), or fumonisin B (*fumon.*), an inhibitor of sphingomyelin and glycosphingolipid biosynthesis, NB-DNJ, a blocker of glycosphingolipid biosynthesis, or mevinolin (*mevin.*), an inhibitor of cholesterol biosynthesis (*B*). *Graphs* represent lengths of the longest neurites and total length of all neurites per neuron (mean values ± S.E., $n > 100$ neurons were analyzed in three independent experiments). Note that CHL1-dependent neurite outgrowth is blocked by the inhibitors. *, $p < 0.05$, one-way ANOVA with Dunnett's multiple comparison test (compared with all other groups). *C,* cultured hippocampal neurons transfected with cherry fluorescent protein or co-transfected with cherry together with CHL1WT or CHL1C1102S were incubated with nonimmune immunoglobulins (*IgG*) or CHL1 antibodies for 24 h. *Graphs* represent lengths of the longest neurite and total lengths of all neurites per neuron (mean values ± S.E., $n > 250$ neurons were analyzed in three independent experiments). Note that overexpression of CHL1C1102S inhibits the response to CHL1 antibodies. Overexpression of CHL1WT slightly reduces overall neurite outgrowth but does not block the ability of neurons to respond to CHL1 antibodies. *, $p < 0.05$, one-way ANOVA with Dunnett's multiple comparison test (compared with cherry-transfected IgG-treated group).

growth (1, 7, 8) and, conversely, by restricting neurite outgrowth and promoting growth cone collapse (2, 12). In this study, we show that the neuritogenesis-promoting functions of CHL1 are induced by ligand-mediated clustering and endocytosis of CHL1. This endocytosis depends on the integrity of lipid rafts and local reorganization of the cytoskeleton regulated by the association of CHL1 with lipid rafts. Mutation of the cysteine residue within the intracellular domain of CHL1 abolishes the association of CHL1 with lipids rafts indicating that palmitoylation plays an important role. Reversible palmitoylation has been shown for a number of proteins in the brain contributing to regulation of their localization and function (32, 33). Our observation that CHL1 is palmitoylated in response to ligand binding suggests that CHL1 can be directly linked to the pathways involved in regulation of palmitoylation-related enzymes. Although the molecular pathways leading to CHL1 palmitoylation remain to be identified, the physiological significance of this post-translational modification is underscored by our data demonstrating that ligand-induced endocytosis of CHL1 with mutated cysteine 1102 is inhibited, and overexpression of this mutant interferes with CHL1 ligand-induced neurite outgrowth.

The triggering of CHL1 functions at the cell surface are transmitted to the cytoskeleton as found in this study. Previous work has determined that CHL1 functionally interacts with the cytoskeleton linker protein ankyrin (3), which in turn binds to the spectrin meshwork (34). Several transmembrane proteins, including cell adhesion molecules, can also bind directly to the spectrin meshwork (18, 34), and we identify βII spectrin as a novel cytoskeletal binding partner of CHL1. Our observations

showing that antibody-induced clustering of CHL1 leads to redistribution of βII spectrin to CHL1 clusters and that high levels of βII spectrin co-immunoprecipitate with CHL1 indicate that CHL1 is one of the major binding partners of βII spectrin at the cell surface plasma membrane. Previous observations had suggested that ankyrins and spectrins can play distinct roles in regulation of endocytosis. Ankyrin binding to clathrin promotes endocytosis via clathrin-coated pits (35), although the spectrin meshwork inhibits endocytosis of cell surface proteins in fibroblasts (36) and in synapses of mature neurons (26). The observations of this study indicate that similar mechanisms are operant in developing neurons with the spectrin meshwork inhibiting ligand-induced endocytosis of CHL1. The disassembly of the CHL1-βII spectrin complex is accompanied by the removal of βII spectrin from the neuronal cell surface, similarly to what has been described for erythrocytes in which the spectrin meshwork is removed before endocytosis occurs (37, 38). Whether interactions of CHL1 with ankyrin and other components of the cytoskeleton, such as ERM family proteins (12), also play a role in CHL1 endocytosis remains to be determined.

Our data indicate that the CHL1-associated spectrin meshwork is disassembled in lipid rafts. Because lipid rafts are enriched in voltage-dependent Ca^{2+} channels (22), CHL1 ligand-induced redistribution of the CHL1-βII spectrin complex to lipid rafts may facilitate Ca^{2+}-dependent disassembly of the complex. Spectrin αII contains Ca^{2+}-binding EF-hands (39) and can bind to calmodulin (40), thus being directly linked to the Ca^{2+} signaling network. An increase in Ca^{2+} may also influence the integrity of the spectrin meshwork by activating the Ca^{2+}-dependent actin-severing protein gelsolin, which is involved in spectrin meshwork remodeling (41). An additional pathway for spectrin meshwork remodeling may include its partial proteolysis, because this meshwork is known to be attacked by Ca^{2+}-dependent proteases during neurite outgrowth (42), a pathway that can be activated by adhesion molecules (43).

Disruption of the CHL1-βII spectrin complex may not only open the territory for endocytic zone formation but also release CHL1 for interactions with endocytic components. It is noteworthy in this context that CHL1 participates in activating clathrin-dependent pathway mechanisms (14). Redistribution of CHL1 to lipid rafts may also link it to lipid raft-enriched endocytic adaptors, such as flotillins, which are involved in endocytosis of cell surface receptors in a lipid raft-dependent manner (44, 45).

The removal of CHL1 from the cell surface might be necessary to attenuate adhesion forces to allow for less rigid cell interactions to occur for neurite outgrowth or for reducing CHL1-dependent growth cone collapse in response to inhibitory signals (12). Yet we do not exclude that CHL1 endocytosis is required for CHL1 recycling, a phenomenon previously described for its close homolog L1 (46, 47). We propose that CHL1 ligands promoting endocytosis of CHL1 tip the balance toward enhancing neuritogenesis, whereas CHL1 ligands not promoting this mechanism tip this balance toward inhibition of neuritogenesis. Overall, our data may explain previous seemingly controversial data indicating that CHL1 not only promotes but also inhibits neurite outgrowth when neurons are engaged in *trans*-interactions with CHL1-expressing astrocytes (2) by a mechanism in which a homophilic *trans*-interaction of CHL1 with CHL1 on adjacent cells may impede CHL1 endocytosis.

Interestingly, CHL1 deficiency results in overall reduced levels of βII spectrin in lipid rafts and increased levels of polymerized βII spectrin in the brain. Thus, an abnormal spectrin meshwork organization is a plausible contributor to the pathological processes occurring in the brains of $CHL1^{-/-}$ mice and humans carrying mutations in the *CHL1* gene (48–51).

Although CHL1 is predominantly targeted to axons in mature hippocampal neurons (14), it is distributed in all neurites and in soma of immature hippocampal neurons as analyzed in this study. Consistent with this broader distribution, CHL1 antibody induces neurite outgrowth not only in putative axons but also in all other neurites indicating that it may contribute to the regulation of overall neuronal morphology at early developmental stages. Previous observations on the abnormal development of apical dendrites in the visual and somatosensory cortex in CHL1-deficient mice (10) are in agreement with this view.

Although reduced CHL1-mediated adhesion appears to be needed to allow neurite outgrowth, CHL1-enforced adhesion may become important at later stages of neuronal development to stabilize synapses where CHL1 accumulates (14, 15). $CHL1^{-/-}$ mice display reduced novelty detection, impaired social behavior, and reduced working memory (48, 49, 52), which have been associated with some symptoms of schizophrenia in humans carrying missense polymorphisms in the *CHL1* gene (50, 51). Whether the association of CHL1 with lipid rafts and βII spectrin is important for synapse formation and function and whether disruption of this link contributes to the etiology of schizophrenia are intriguing questions deserving further investigation.

Acknowledgments—We thank Dr. Roger Tsien (University of California at San Diego) for the cherry construct. We are also grateful to Ute Eicke-Kohlmorgen, Achim Dahlmann, and Eva Kronberg for technical assistance, genotyping, and animal care.

REFERENCES

1. Hillenbrand, R., Molthagen, M., Montag, D., and Schachner, M. (1999) The close homologue of the neural adhesion molecule L1 (CHL1). Patterns of expression and promotion of neurite outgrowth by heterophilic interactions. *Eur. J. Neurosci.* **11,** 813–826
2. Jakovcevski, I., Wu, J., Karl, N., Leshchyns'ka, I., Sytnyk, V., Chen, J., Irintchev, A., and Schachner, M. (2007) Glial scar expression of CHL1, the close homolog of the adhesion molecule L1, limits recovery after spinal cord injury. *J. Neurosci.* **27,** 7222–7233
3. Buhusi, M., Midkiff, B. R., Gates, A. M., Richter, M., Schachner, M., and Maness, P. F. (2003) Close homolog of L1 is an enhancer of integrin-mediated cell migration. *J. Biol. Chem.* **278,** 25024–25031
4. Ye, H., Tan, Y. L., Ponniah, S., Takeda, Y., Wang, S. Q., Schachner, M., Watanabe, K., Pallen, C. J., and Xiao, Z. C. (2008) Neural recognition molecules CHL1 and NB-3 regulate apical dendrite orientation in the neocortex via PTPα. *EMBO J.* **27,** 188–200
5. Wright, A. G., Demyanenko, G. P., Powell, A., Schachner, M., Enriquez-Barreto, L., Tran, T. S., Polleux, F., and Maness, P. F. (2007) Close homolog of L1 and neuropilin 1 mediate guidance of thalamocortical axons at the ventral telencephalon. *J. Neurosci.* **27,** 13667–13679

6. Demyanenko, G. P., Siesser, P. F., Wright, A. G., Brennaman, L. H., Bartsch, U., Schachner, M., and Maness, P. F. (2011) L1 and CHL1 cooperate in thalamocortical axon targeting. *Cereb. Cortex* **21,** 401–412
7. Nishimune, H., Bernreuther, C., Carroll, P., Chen, S., Schachner, M., and Henderson, C. E. (2005) Neural adhesion molecules L1 and CHL1 are survival factors for motoneurons. *J. Neurosci. Res.* **80,** 593–599
8. Chen, S., Mantei, N., Dong, L., and Schachner, M. (1999) Prevention of neuronal cell death by neural adhesion molecules L1 and CHL1. *J. Neurobiol.* **38,** 428–439
9. Jakovcevski, I., Siering, J., Hargus, G., Karl, N., Hoelters, L., Djogo, N., Yin, S., Zecevic, N., Schachner, M., and Irintchev, A. (2009) Close homologue of adhesion molecule L1 promotes survival of Purkinje and granule cells and granule cell migration during murine cerebellar development. *J. Comp. Neurol.* **513,** 496–510
10. Demyanenko, G. P., Schachner, M., Anton, E., Schmid, R., Feng, G., Sanes, J., and Maness, P. F. (2004) Close homolog of L1 modulates area-specific neuronal positioning and dendrite orientation in the cerebral cortex. *Neuron* **44,** 423–437
11. Ango, F., Wu, C., Van der Want, J. J., Wu, P., Schachner, M., and Huang, Z. J. (2008) Bergmann glia and the recognition molecule CHL1 organize GABAergic axons and direct innervation of Purkinje cell dendrites. *PLoS Biol.* **6,** e103
12. Schlatter, M. C., Buhusi, M., Wright, A. G., and Maness, P. F. (2008) CHL1 promotes Sema3A-induced growth cone collapse and neurite elaboration through a motif required for recruitment of ERM proteins to the plasma membrane. *J. Neurochem.* **104,** 731–744
13. Naus, S., Richter, M., Wildeboer, D., Moss, M., Schachner, M., and Bartsch, J. W. (2004) Ectodomain shedding of the neural recognition molecule CHL1 by the metalloprotease-disintegrin ADAM8 promotes neurite outgrowth and suppresses neuronal cell death. *J. Biol. Chem.* **279,** 16083–16090
14. Leshchyns'ka, I., Sytnyk, V., Richter, M., Andreyeva, A., Puchkov, D., and Schachner, M. (2006) The adhesion molecule CHL1 regulates uncoating of clathrin-coated synaptic vesicles. *Neuron* **52,** 1011–1025
15. Andreyeva, A., Leshchyns'ka, I., Knepper, M., Betzel, C., Redecke, L., Sytnyk, V., and Schachner, M. (2010) CHL1 is a selective organizer of the presynaptic machinery chaperoning the SNARE complex. *PLoS ONE* **5,** e12018
16. Montag-Sallaz, M., Schachner, M., and Montag, D. (2002) Misguided axonal projections, neural cell adhesion molecule 180 mRNA up-regulation, and altered behavior in mice deficient for the close homolog of L1. *Mol. Cell. Biol.* **22,** 7967–7981
17. Bennett, V., Baines, A. J., and Davis, J. (1986) Purification of brain analogs of red blood cell membrane skeletal proteins: ankyrin, protein 4.1 (synapsin), spectrin, and spectrin subunits. *Methods Enzymol.* **134,** 55–69
18. Leshchyns'ka, I., Sytnyk, V., Morrow, J. S., and Schachner, M. (2003) Neural cell adhesion molecule (NCAM) association with PKCβ2 via βI spectrin is implicated in NCAM-mediated neurite outgrowth. *J. Cell Biol.* **161,** 625–639
19. Molitoris, B. A., Dahl, R., and Hosford, M. (1996) Cellular ATP depletion induces disruption of the spectrin cytoskeletal network. *Am. J. Physiol.* **271,** F790–F798
20. Devanathan, V., Jakovcevski, I., Santuccione, A., Li, S., Lee, H. J., Peles, E., Leshchyns'ka, I., Sytnyk, V., and Schachner, M. (2010) Cellular form of prion protein inhibits Reelin-mediated shedding of Caspr from the neuronal cell surface to potentiate Caspr-mediated inhibition of neurite outgrowth. *J. Neurosci.* **30,** 9292–9305
21. Chernyshova, Y., Leshchyns'ka, I., Hsu, S. C., Schachner, M., and Sytnyk, V. (2011) The neural cell adhesion molecule promotes FGFR-dependent phosphorylation and membrane targeting of the exocyst complex to induce exocytosis in growth cones. *J. Neurosci.* **31,** 3522–3535
22. Bodrikov, V., Sytnyk, V., Leshchyns'ka, I., den Hertog, J., and Schachner, M. (2008) NCAM induces CaMKIIα-mediated RPTPα phosphorylation to enhance its catalytic activity and neurite outgrowth. *J. Cell Biol.* **182,** 1185–1200
23. Bodrikov, V., Leshchyns'ka, I., Sytnyk, V., Overvoorde, J., den Hertog, J., and Schachner, M. (2005) RPTPα is essential for NCAM-mediated p59fyn activation and neurite elongation. *J. Cell Biol.* **168,** 127–139
24. Nakai, Y., and Kamiguchi, H. (2002) Migration of nerve growth cones requires detergent-resistant membranes in a spatially defined and substrate-dependent manner. *J. Cell Biol.* **159,** 1097–1108
25. Sytnyk, V., Leshchyns'ka, I., Delling, M., Dityateva, G., Dityatev, A., and Schachner, M. (2002) Neural cell adhesion molecule promotes accumulation of TGN organelles at sites of neuron-to-neuron contacts. *J. Cell Biol.* **159,** 649–661
26. Puchkov, D., Leshchyns'ka, I., Nikonenko, A. G., Schachner, M., and Sytnyk, V. (2011) NCAM/spectrin complex disassembly results in PSD perforation and postsynaptic endocytic zone formation. *Cereb. Cortex* **21,** 2217–2232
27. Du, X., Kumar, J., Ferguson, C., Schulz, T. A., Ong, Y. S., Hong, W., Prinz, W. A., Parton, R. G., Brown, A. J., and Yang, H. (2011) A role for oxysterol-binding protein-related protein 5 in endosomal cholesterol trafficking. *J. Cell Biol.* **192,** 121–135
28. Niethammer, P., Delling, M., Sytnyk, V., Dityatev, A., Fukami, K., and Schachner, M. (2002) Cosignaling of NCAM via lipid rafts and the FGF receptor is required for neuritogenesis. *J. Cell Biol.* **157,** 521–532
29. Ponimaskin, E., Dityateva, G., Ruonala, M. O., Fukata, M., Fukata, Y., Kobe, F., Wouters, F. S., Delling, M., Bredt, D. S., Schachner, M., and Dityatev, A. (2008) Fibroblast growth factor-regulated palmitoylation of the neural cell adhesion molecule determines neuronal morphogenesis. *J. Neurosci.* **28,** 8897–8907
30. De Matteis, M. A., and Morrow, J. S. (2000) Spectrin tethers and mesh in the biosynthetic pathway. *J. Cell Sci.* **113,** 2331–2343
31. Laux, T., Fukami, K., Thelen, M., Golub, T., Frey, D., and Caroni, P. (2000) GAP43, MARCKS, and CAP23 modulate PI(4,5)P_2 at plasmalemmal rafts and regulate cell cortex actin dynamics through a common mechanism. *J. Cell Biol.* **149,** 1455–1472
32. Kang, R., Wan, J., Arstikaitis, P., Takahashi, H., Huang, K., Bailey, A. O., Thompson, J. X., Roth, A. F., Drisdel, R. C., Mastro, R., Green, W. N., Yates, J. R., 3rd, Davis, N. G., and El-Husseini, A. (2008) Neural palmitoyl-proteomics reveals dynamic synaptic palmitoylation. *Nature* **456,** 904–909
33. Fukata, Y., and Fukata, M. (2010) Protein palmitoylation in neuronal development and synaptic plasticity. *Nat. Rev. Neurosci.* **11,** 161–175
34. Bennett, V., and Healy, J. (2009) Membrane domains based on ankyrin and spectrin associated with cell-cell interactions. *Cold Spring Harbor Perspect. Biol.* **1,** a003012
35. Michaely, P., Kamal, A., Anderson, R. G., and Bennett, V. (1999) A requirement for ankyrin binding to clathrin during coated pit budding. *J. Biol. Chem.* **274,** 35908–35913
36. Kamal, A., Ying, Y., and Anderson, R. G. (1998) Annexin VI-mediated loss of spectrin during coated pit budding is coupled to delivery of LDL to lysosomes. *J. Cell Biol.* **142,** 937–947
37. Hardy, B., Bensch, K. G., and Schrier, S. L. (1979) Spectrin rearrangement early in erythrocyte ghost endocytosis. *J. Cell Biol.* **82,** 654–663
38. Schrier, S. L., Hardy, B., and Bensch, K. G. (1979) Endocytosis in erythrocytes and their ghosts. *Prog. Clin. Biol. Res.* **30,** 437–449
39. Travé, G., Pastore, A., Hyvönen, M., and Saraste, M. (1995) The C-terminal domain of α-spectrin is structurally related to calmodulin. *Eur. J. Biochem.* **227,** 35–42
40. Simonovic, M., Zhang, Z., Cianci, C. D., Steitz, T. A., and Morrow, J. S. (2006) Structure of the calmodulin αII-spectrin complex provides insight into the regulation of cell plasticity. *J. Biol. Chem.* **281,** 34333–34340
41. Hinssen, H., Vandekerckhove, J., and Lazarides, E. (1987) Gelsolin is expressed in early erythroid progenitor cells and negatively regulated during erythropoiesis. *J. Cell Biol.* **105,** 1425–1433
42. Spira, M. E., Oren, R., Dormann, A., Ilouz, N., and Lev, S. (2001) Calcium, protease activation, and cytoskeleton remodeling underlie growth cone formation and neuronal regeneration. *Cell. Mol. Neurobiol.* **21,** 591–604
43. Westphal, D., Sytnyk, V., Schachner, M., and Leshchyns'ka, I. (2010) Clustering of the neural cell adhesion molecule (NCAM) at the neuronal cell surface induces caspase-8- and -3-dependent changes of the spectrin meshwork required for NCAM-mediated neurite outgrowth. *J. Biol. Chem.* **285,** 42046–42057
44. Schneider, A., Rajendran, L., Honsho, M., Gralle, M., Donnert, G., Wouters, F., Hell, S. W., and Simons, M. (2008) Flotillin-dependent clustering of

the amyloid precursor protein regulates its endocytosis and amyloidogenic processing in neurons. *J. Neurosci.* **28,** 2874–2882
45. Stuermer, C. A. (2011) Reggie/flotillin and the targeted delivery of cargo. *J. Neurochem.* **116,** 708–713
46. Kamiguchi, H., and Lemmon, V. (2000) Recycling of the cell adhesion molecule L1 in axonal growth cones. *J. Neurosci.* **20,** 3676–3686
47. Dequidt, C., Danglot, L., Alberts, P., Galli, T., Choquet, D., and Thoumine, O. (2007) Fast turnover of L1 adhesions in neuronal growth cones involving both surface diffusion and exo/endocytosis of L1 molecules. *Mol. Biol. Cell* **18,** 3131–3143
48. Morellini, F., Lepsveridze, E., Kähler, B., Dityatev, A., and Schachner, M. (2007) Reduced reactivity to novelty, impaired social behavior, and enhanced basal synaptic excitatory activity in perforant path projections to the dentate gyrus in young adult mice deficient in the neural cell adhesion molecule CHL1. *Mol. Cell. Neurosci.* **34,** 121–136
49. Pratte, M., and Jamon, M. (2009) Impairment of novelty detection in mice targeted for the *Chl1* gene. *Physiol. Behav.* **97,** 394–400
50. Sakurai, K., Migita, O., Toru, M., and Arinami, T. (2002) An association between a missense polymorphism in the close homologue of L1 (CHL1, CALL) gene and schizophrenia. *Mol. Psychiatry* **7,** 412–415
51. Chen, Q. Y., Chen, Q., Feng, G. Y., Lindpaintner, K., Chen, Y., Sun, X., Chen, Z., Gao, Z., Tang, J., and He, L. (2005) Case-control association study of the close homologue of L1 (CHL1) gene and schizophrenia in the Chinese population. *Schizophr. Res.* **73,** 269–274
52. Kolata, S., Wu, J., Light, K., Schachner, M., and Matzel, L. D. (2008) Impaired working memory duration but normal learning abilities found in mice that are conditionally deficient in the close homolog of L1. *J. Neurosci.* **28,** 13505–13510